



Coupling Between Fluid-Flow and Mechanics Simulation for
Hydrocarbon Reservoir Analysis

Turin, Italy

December 2018

Department of Environment, Land and Infrastructure Engineering

In partial fulfillment of the requirements for the degree of Master of
Science in Petroleum Engineering

Submitted by:

Georges El Debs

Advisor:

Prof. Vera Rocca

Acknowledgement

I would like to dedicate this paper to my family and my friends for always believing in me and always being by my side. I promise to keep on making you proud and to always meet the expectations and more.

Firstly, I would like to thank Professor Vera Rocca for being a great advisor and teacher throughout the past couple of years. I'm confident that Professor Rocca will also continue to be a reliable mentor for me even after this journey is over.

I would also like to express my deep gratitude for all the factors that brought me here to Italy generally and Turin specifically, since the year I spent here were without any doubt the best years of my life. I would also like to thank Politecnico for this amazing journey and the life-changing experiences it put me through.

Last but not least, I would like to thank all my professors for their dedication, it was an honor to share this experience with each of you.

Abstract

Reservoir fluid flow and reservoir rock deformation due to production have been standardly handled as two separate issues for oil and gas reservoir development, on the basis of simplified assumption on interaction between different phenomena. While reservoir rock displacement has been primarily used for surface subsidence severity simulations, it is well known that in particular cases (such as shallow purely consolidated hydrocarbon bearing formations) reservoir rock deformation also has an effect on the reservoir's petrophysical properties. Consequently, this effect on petrophysical properties could be severe enough to affect fluid flow behavior and can cause significant changes in reservoir productivity. This issue paved the way for the creation of models that could couple reservoir fluid flow simulations with reservoir geomechanical simulations in order to update petrophysical properties, mainly porosity and permeability, in order to monitor how this change could affect reservoir production capabilities. In this paper, two synthetic cases representing standard off shore Adriatic gas bearing formation at different depths will be simulated using Eclipse on one hand for production data generation and on the other hand one way and two way coupling simulations will be run on Visage finite element simulator through Petrel. The objective of the thesis is to test the different coupling methods on each case in order to evaluate the effect of permeability decrease on production data and to also monitor subsidence results variation between the different two way coupling methods and the one way coupling simulation.

Table of Contents

Chapter 1: Introduction..... 1

Chapter 2: Theoretical Background of coupling fluid flow & stress strain phenomena 3

 Biot’s Theory 3

 Reservoir Simulators and Stress Models..... 4

 Coupling Methods 5

 Coupling Laws..... 7

Chapter 3: Case Study Results and Comments 9

 Case 1..... 9

 Reservoir Production Data..... 10

 Scenario 1..... 11

 Scenario 2..... 13

 One Way Coupling..... 16

 Reservoir Geomechanics Simulation Data..... 16

 Subsidence Analysis..... 19

 Two Way Coupling..... 22

 Kozeny-Carman..... 22

 Polynomial Law..... 26

 Intact Porosity Table..... 30

 Case 2..... 33

 Reservoir Production Data..... 34

 One Way Coupling..... 37

 Reservoir Geomechanics Simulation Data..... 37

 Subsidence Analysis..... 39

 Two Way Coupling..... 42

 Kozeny-Carman..... 42

 Polynomial Law..... 45

 Intact Porosity Table..... 48

Chapter 4: Discussion and Comparison..... 52

 Subsidence 52

 Production Data 55

Chapter 5: Conclusion 57

Table of Figures:

Figure 1 Consequences of Subsidence in Gas Reservoirs 2

Figure 2 One Way Coupling..... 6

Figure 3 Iterative Coupling..... 7

Figure 4 Reservoir Pressure Distribution before Production 10

Figure 5 Pressure Decline Curve (case 1)..... 11

Figure 6 Reservoir Pressure Distribution at the end of production (case1) 12

Figure 7 Cumulative Gas Production Rate (case 1)..... 12

Figure 8 Gas Remaining in Place (case 1) 13

Figure 9 Pressure Decline Curve (case 2)..... 14

Figure 10 Reservoir Pressure Distribution at the end of production (case 2)..... 14

Figure 11 Cumulative Gas Production with respect to Time (scenario 2)..... 15

Figure 12 Remaining Gas in Place with respect to time (scenario 2)..... 15

Figure 13 Legend showing rock displacement intensity in millimeters for figures 13 and 16..... 17

Figure 14 Rock Vertical Displacement in the Reservoir at the end of production in millimeters 17

Figure 15 Rock Vertical Displacement in the reservoir as a function of Time 18

Figure 16 Pressure Decline Curve 18

Figure 17 Rock vertical Displacement on the Surface..... 19

Figure 18 Surface Vertical Rock Displacement..... 20

Figure 19 Rock Vertical Displacement at the Surface with respect to Time..... 20

Figure 20 Rock Lateral Displacement with respect to Time 21

Figure 21 Permeability Decline Kozeny-Carman..... 23

Figure 22 Remaining Gas in Place with respect to time One Way (Red) vs Kozeny-Carman (Green) 24

Figure 23 Cumulative Gas Production with respect to Time One Way (Red) vs Kozeny-Carman (Green) 24

Figure 24 Pressure Decline Curve One Way (Red) vs Kozeny-Carman (Green)..... 25

Figure 25 Permeability Decline Polynomial Law..... 26

Figure 26 Remaining Gas in Place with respect to time One Way (Red) Polynomial Law (Green) 27

Figure 27 Cumulative Gas Production with respect to Time One Way (Red) Polynomial Law (Green) 28

Figure 28 Pressure Decline Curve One Way (Red) Polynomial Law (Green) 28

Figure 29 Data from Lab..... 29

Figure 30 Permeability Decline Intact Porosity Table..... 30

Figure 31 Remaining Gas in Place with respect to time One Way (Red) vs Intact Porosity (Green) 31

Figure 32 Cumulative Gas Production with respect to Time One Way (Red) vs Intact Porosity (Green) 31

Figure 33 Pressure Decline Curve One Way (Red) vs Intact Porosity (Green)..... 32

Figure 34 Pressure Distribution Case 1 33

Figure 35 Pressure Decline Curve One Way Coupling 34

Figure 36 Cumulative Gas Production with respect to Time One Way Coupling.....	35
Figure 37 Remaining Gas in Place with respect to time One Way Coupling.....	35
Figure 38 Legend showing intensity of Rock Displacement in millimeters for figures 37 40 and 42.....	36
Figure 39 Rock Vertical Displacement in the Reservoir	37
Figure 40 Reservoir Rock Vertical Displacement with respect to Time	37
Figure 41 Pressure Decline Curve	38
Figure 42 Surface Subsidence.....	39
Figure 43 Surface Vertical Rock Displacement with respect to Time.....	39
Figure 44 Rock Displacement in the Horizontal Direction	40
Figure 45 Rock Horizontal Displacement with respect to Time.....	40
Figure 46 Permeability Decline Kozeny-Carman.....	42
Figure 47 Remaining Gas in Place with respect to time One Way Coupling (RED) Kozeny Carman (GREEN).....	43
Figure 48 Cumulative Gas Production with respect to Time One Way Coupling (RED) Kozeny Carman (GREEN).....	43
Figure 49 Pressure Decline Curve One Way Coupling (RED) Kozeny Carman (GREEN).....	44
Figure 50 Permeability Decline Polynomial Law.....	45
Figure 51 Remaining Gas in Place with respect to time One Way Coupling (RED) Polynomial Law (GREEN)	45
Figure 52 Cumulative Gas Production with respect to Time One Way Coupling (RED) Polynomial Law (GREEN).....	46
Figure 53 Pressure Decline Curve One Way Coupling (RED) Polynomial Law (GREEN)	47
Figure 54 Permeability Decline Intact Porosity Table.....	48
Figure 55 Remaining Gas in Place with respect to time One Way Coupling (RED) Intact Porosity Table (Green).....	49
Figure 56 Cumulative Gas Production with respect to Time One Way Coupling (RED) Intact Porosity Table (Green).....	50
Figure 57 Pressure Decline Curve One Way Coupling (RED) Intact Porosity Table (Green).....	50
Figure 58 Surface Subsidence For all Coupling Methods	51
Figure 59 Surface Subsidence Results For Each Coupling Method	52
Figure 60 Surface Subsidence 300m vs 1500m.....	53
Figure 61 Case 1 Surface Subsidence Radius vs Case 2 Surface Subsidence Radius.....	54
Figure 62 Subsidence Representation.....	54

Tables:

Table 1 Medium Depth Reservoir Rock Displacement vs Surface Subsidence vs Subsidence Impact Radius	21
Table 2 Shallow Depth Reservoir Rock Displacement vs Surface Subsidence vs Subsidence Impact Radius	41
Table 3 Permeability Percent Change at the end of production.....	55
Table 4 Percent Decrease in Recovery Factor	55

Nomenclature:

σ_{ij} : Effective Stress

σ'_{ij} : Total Stress

σ_m : Mean Stress

α : Biot's Principle

P_p : Pore Pressure

k : Permeability

K_b : Bulk Permeability

k_0 : Initial Permeability

μ : Viscosity

t : Time

\emptyset : Porosity

C_b : Bulk Compressibility

C_s : Solid Compressibility

C_p : Rock Compressibility Pressure Coefficient

e : Young Modulus

λ : Lamé's Constant

G : Shear Modulus

i : Iteration level

n : time step

ε_v : Volumetric Strain

$\varepsilon_x, \varepsilon_y, \varepsilon_z$: Axial Strain

List of Equations

Equation 1	4
Equation 2	4
Equation 3	4
Equation 4	4
Equation 5	4
Equation 6	8
Equation 7	8
Equation 8	8
Equation 9	8
Equation 10	9
Equation 11	9
Equation 12	9
Equation 13	22
Equation 14	22

Chapter 1: Introduction

Whether we are talking about oil and gas reservoir production or environmental soil reclamation, these processes cause an interaction between fluid flow and heat transfer with stress and strain behavior in the reservoir. The interaction between two or more of the above mentioned phenomena interest different fields of investigations, for example compaction due to production and loss of pressure of fluids in porous media, steam injection which will cause heat transfer and increase in pressure, fracture propagation while water flooding, cleanup operations of contaminated shallow water reservoirs ^[1] and chemicals injection such as polymers or CO_2 . Previously, there was no single modeling platform that can automatically perform coupling of fluid flow and the geomechanical issues. Currently, some platforms were created to handle this issue but they are very complex and time consuming. Coupling is performed usually on three different models; reservoir simulation which deals with modeling fluid flow and heat transfer, geomechanical modeling which deals with stress and strain behavior, and fracture propagation modeling which deals with fracture geometry and enlargement ^[1]. Each of these modeling and simulation platforms automatically makes assumptions that allows them to perform their objective while discarding the other part of the problem which is not in their priority interest ^[1]. While this is a reasonable assumption in a lot of cases, it cannot be acceptable in cases where there is a strong relationship between two or more phenomena. The main focus of the thesis is to understand how important the effect of coupling between a reservoir simulator and a geomechanical simulator is on production data and geomechanical data, while analyzing the results obtained when applying the different methods of two way coupling simulations and the one way coupling simulations. Consequently, on one hand we will study the effects of production and reservoir compaction on subsidence and on the other hand the effects that reservoir rock displacement could bring on reservoir fluid flow.

Surface subsidence has been a very important issue lately due to safety reasons. Depending on the typology of the reservoir rock, the depth, the shape and the deformation features of the reservoir formation and the typologies of rock above the reservoir in addition to the induced pressure variation, the degree of rock displacement can be determined as well as surface subsidence analytical or numerical approaches. Surface subsidence intensity is a very important issue to determine, since it could cause a lot of damages on the surface facilities and on surrounding habitable areas. This damage could lead to losses of equipment and could also put the lives of the ones in that area in danger. In Italy for example, the first significant subsidence issue caused by gas production took place in the late 1950s in the Po River Delta area, due to the uncontrolled production of a shallow gas formations at a depth between 100 and 600 meters ^[2]. The subsidence levels were on average 1 meter while it reached in some areas up to 3 meters. This resulted in several environmental problems, from “marine ingressions to damages to the river embankments, making the area more predisposed to river flooding” ^[2].

In addition, in the case of gas reservoirs, if rock displacement in the reservoir causes fault formations and fractures underground at the reservoir level, this could lead to gas migrations to the surface which could lead to explosions ^[3].

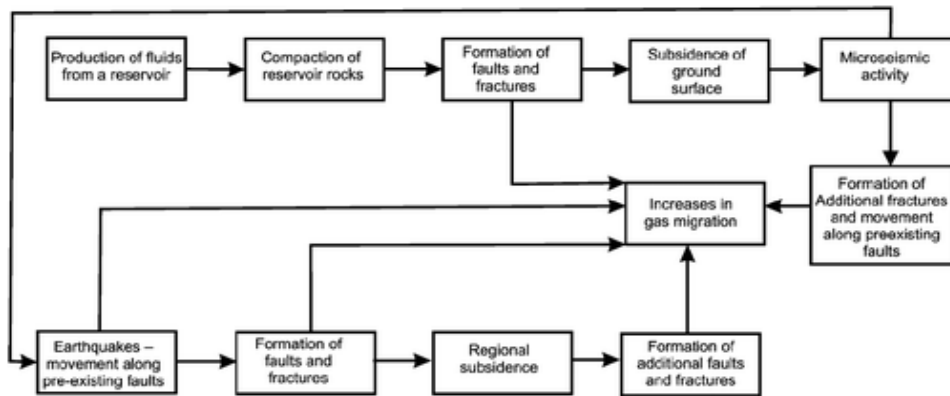


Figure 1 Consequences of Subsidence in Gas Reservoirs [3]

Reservoir engineering has been developed for quite a long time to model different types of reservoirs in order to understand their behavior during and after the production period [4]. In reservoir simulation it is always important to understand the factors that affect fluid flow in the reservoir and since in many conventional cases, the interaction between stress-strain and fluid flow is very limited, for a long time geo-mechanical compaction has not been taken into account regarding its effect on fluid flow. However, in other cases, interactions between fluid flow and stress/strain behavior in the porous media take place significantly, which can consequently affect reservoir production performance and productivity. In cases where the interaction between these two factors is strongly existent and in order to simulate production and geomechanical data correctly, two way coupling solutions must be implemented. Therefore, it is important to find and exploit a relationship between reservoir compaction and fluid flow in a given reservoir in order to recognize these interactions and to identify how significant these interactions are. Coupling of reservoir simulators with stress models offers us the opportunity to make the link between reservoir properties and reservoir compaction. This could help us determine how reservoir permeability and porosity is affected by stress and strain during production thus affecting our reservoir's fluid flow. The focus of this study is on permeability and porosity, consequently fluid flow.

During the lifecycle of a reservoir, porosity and absolute permeability may change in response to changes in stress within the porous media due to the pressure drop during production time [1]. The pressure drop can induce an increase in net effective stress consequently altering pore geometry of the reservoir rock. This change will thus cause a drop in permeability and porosity, which might consequently affect the reservoir's fluid flow, knowing that the rate of change of permeability from one case to another varies widely [5]. In this paper, we will be testing out several coupling methods on two different reservoir cases. The aim is to understand the degree of importance of the different coupling methods on subsidence simulation as well as production forecast and to determine what kind of studies are still missing in order to make these coupling solutions reliable for all different reservoir cases.

The bulk of the thesis is composed of three different sections:

- The first section represented by the second chapter discusses Biot's theory which describes fluid and solid interaction, the introduction to the coupling approach where the simulators are briefly explained and the coupling techniques are introduced as well as porosity relation to stress/strain and permeability relations to porosity changes.
- The second section represented by the third chapter will be the core of this paper, where two case studies will be exploited along with their results. The two studies were performed on two synthetic in the Adriatic Sea, case 1 being a medium depth sandstone reservoir at 1500 m depth and case 2 being a shallow reservoir with poorly consolidated sandstone at 300 m depth with the same petrophysical properties as case 1. The coupling was performed between a standard reservoir simulator ECLIPS and a geomechanical simulator within PETREL called VISAGE. Each case study will be split into two basic parts, the first one is one way coupling meant to determine subsidence issues and the other part is iterative coupling meant to analyze the effect of compaction on reservoir fluid flow.
- The fourth chapter will cover all the details witnessed in the results represented in chapter three along with the comparison between the two case studies where possible.

Chapter 2: Theoretical Background of coupling fluid flow & stress strain phenomena

A- Biot's theory and diffusivity equation - basics:

When dealing with reservoir engineering problems, one must always involve the two most important elements; fluid phenomena and rock deformation. The theory describing fluid and solid interaction, in other words coupling, is called the poroelastic theory and was first introduced by Biot ^[6]. When dealing with Biot it is a must to start with the principle of effective stress, first developed by Terzaghi, who considered that soil is confined and only undergoes uniaxial consolidation, and rock and fluid are incompressible. Terzaghi's effective stress principle was a breakthrough since it was the first solution for the consolidation problem. In this theory, it is stated that the applied stress is transmitted to the pore fluid content and to the rock matrix. The stress transmitted to the pore fluid can induce a pressure gradient with consequent effects on fluid flow, while the stress applied to the skeleton causes deformation as a result.

Later on, Biot introduced three dimensional theory of elastic deformation on fluid saturated porous media, where both solid and fluid are compressible. Solid phase is compressible and is not necessarily composed of a single constituent. Pore fluid is compressible and consists of a single phase. The theory was also further developed to anisotropic elastic formations, and nonlinear elasticity. Mass balance is a basic fundamental component to account for fluid flow which is considered as a viscous fluid which flows Darcy's law ^[6].

The effective stress principle states that when the rock is subjected to stress it is opposed by pore fluid pressure. Consequently, all changes in stress to a rock are directly related to

changes in effective stress. The relationship between effective stress, total stress and pore pressure are demonstrated in the equation below:

$$\sigma_{ij} = \sigma'_{ij} - \alpha P_p \quad [6] \dots\dots\dots (1)$$

α is known as Biot's coefficient, Terzaghi took it as 1, which is only valid in the case of soils [5].

Mathematical models that describe the flow of fluids through porous and permeable media are described by merging conservation equations with equations of motion and equations of state. It could be the flow of a single fluid developed using a partial differential equation, or a similar equation could also be developed for multiphase flow [6].

Diffusivity equation:

$$\nabla \cdot \left(\frac{k}{\mu} \nabla p \right) = \phi C_t \frac{\partial p}{\partial t} + (C_b - C_s) \frac{\partial \sigma_m}{\partial t} \quad [7] \dots\dots\dots (2)$$

The linear poroelastic theory, developed by Biot, is the basis for fluid-solid coupling as stated before. Perfectly elastic, limited strains and isothermal conditions are assumed. This theory has three basic principles, which are coherent with the mathematical models that describe fluid flow. These principles are; stress equilibrium, strain vs displacement and strain/stress vs pressure relations.

Using these principles, we get:

$$e = \frac{\sigma_m + \alpha p}{\lambda + \left(\frac{2}{3}\right)G} = \frac{\sigma_m + \alpha p}{K_b} \quad [7] \dots\dots\dots (3)$$

The coupled equations are:

$$\nabla \cdot \left(\frac{k}{\mu} \nabla p \right) = \phi C_t \frac{\partial p}{\partial t} + \alpha \frac{\partial e}{\partial t} \quad [7] \dots\dots\dots (4)$$

$$G \nabla^2 u + (G + \lambda) \nabla \nabla \cdot u = \alpha \nabla p \quad \text{or} \quad (\lambda + 2G) \nabla^2 e = \alpha \nabla^2 p \quad [7] \dots\dots\dots (5)$$

B- Reservoir Simulators and Stress Models

Before we go deeply into the coupling topic, one must understand the two different simulators that are being used for coupling; Reservoir simulators and Stress Models

Reservoir simulators

Reservoir simulators are one of the most useful technologies used in reservoir modeling and it is used to develop fluid flow and heat transfer in porous media. It is able to model multiphase flow reservoirs that could be miscible or immiscible. PVT data inserted can range to different oils with different properties. The fluid characteristics are usually described by PVT, relative permeability and flow history. Stress variation is usually not accounted for using these simulators [1]. "ECLIPSE is a reservoir simulator that provides

the industry's most integrated and sturdy set of numerical solutions for rapid and rigorous simulation of the dynamic behavior of fluids in all different varieties of reservoirs. The ECLIPSE simulator is able to work on the different aspects of reservoir simulation; black oil, compositional, thermal and streamline simulation" [8].

Stress models

Stress models for reservoir formations typically use the theory of consolidation to simulate geomechanical problems. The majority of rock materials could be represented including hard and granular material. Stress models incorporate different element shapes and degree of approximation. Mostly all stress models use the finite element approach for completing for their calculations. [1]"Petrel Reservoir Geomechanics is a software package that is consisted of the VISAGE finite element simulator and the Petrel module. It offers a concrete, versatile, flexible and manually controlled platform for solving a number of complicated engineering problems encountered in the petroleum industry. Dynamic and efficient, the system can be integrates to solve subsidence, compaction and pore collapse problems due to high pressure drop during the production phase. Coupling multiphase reservoir simulations can be applied, linking Petrel Reservoir Geomechanics to ECLIPSE reservoir simulator. This simulator incorporates the disciplines of porous media rock mechanics and petroleum reservoir engineering to predict and calculate the effect of rock deformation on reservoir fluid flow characteristics. Sophisticated 3D reservoir models with complex pre-defined distributions of faults are readily accommodated" [8].

C- Coupling methods

Previously, modeling was only performed on upgraded or improved reservoir simulators. Coupling has proved useful when talking about subsidence problems when considering explicit or one way coupling. On the other hand, data supporting the importance of stress/strain and fracture propagation and behavior surfaced thus making it a must to take geomechanical problems into consideration, a system which relates stress/strain and fracture mechanics with fluid flow in the porous media should be developed. There has always been an interaction between fluid flow and reservoir rock deformation phenomenon. In some cases, where the rock has very low compressibility, this interaction is negligible, while in other cases where high compressibility leads to high volumetric strains this interaction could be seen as significant. Coupling the parameters between these different simulators and models can be done using different coupling methods for different coupling purposes.

Explicit coupling or one way coupling, as discussed before, this method has been basically used for subsidence determination problems. Explicit coupling is an integrated system which allows for the rock stress and strain determination and calculation on a different timescale than the one for fluid flow computations, making it very useful for subsidence problems since it allows the geomechanical calculations to take a big portion of the simulation time. This is ideal for subsidence problems since fluid flow

characteristics and well performance problems may change very quickly, while subsidence develops very slowly compared to the time frame of the simulation [4].

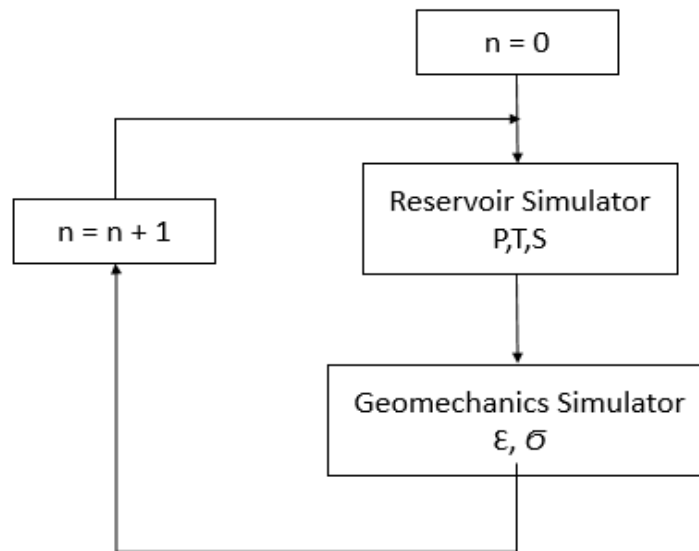


Figure 2 One Way Coupling

Iterative coupling is done by solving fluid flow variables and geomechanical variables separately using reservoir simulators and stress models or fracture propagation models respectively. Consequently, an iterative coupling is performed for each time step reached. The coupling is performed using the pressure and stress changes from the previous two iteration solutions. The goal of the iterative coupling is to see the effect of the pressure drop at each time step calculated by the reservoir simulator on the reservoir's stress and strain, thus altering porosity and/or permeability which could consequently cause a change in reservoir fluid flow behavior [8].

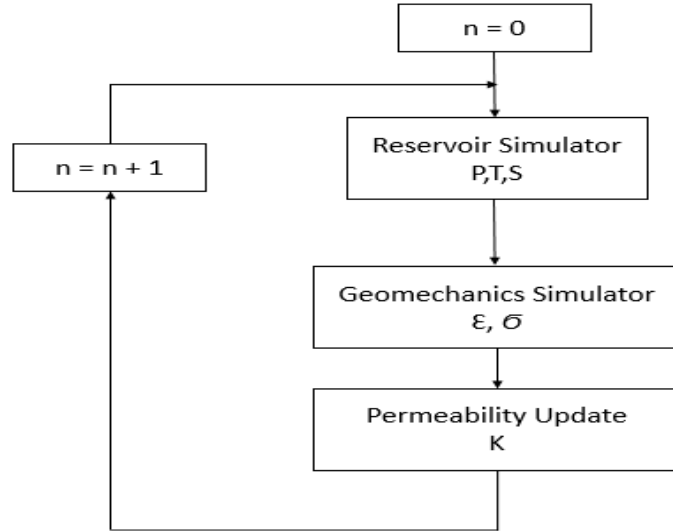


Figure 3 Iterative Coupling

Pseudo Coupling for this type of coupling, reservoir simulators are used to calculate geomechanical responses based on simple equations that relate porosity and strain to obtain compaction and horizontal stress changes. On the other hand, porosity and permeability are updated using models with respect to pressure^[8].

Fully coupling for this coupling method, all petrophysical properties and fluid flow properties are calculated in addition to the geomechanical response simultaneously through a series of equations having all variables needed as unknowns. “This type of coupling has the advantage of internal consistency since it can be solved simultaneously with the same discretization (usually finite element)”^[4].

D- Coupling laws

Volume and Flow Properties coupling

Volume coupling is how changes in pore volume due to stress changes is expressed. Both reservoir simulators and stress models use pore volume changes as an essential input. Pore volume changes are a function of pressure temperature and stress when it comes to coupling. When coupling is not applied, the assumption is that stress changes do not have a significant effect on pore volume changes as pressure and temperature do, but that is not the case where effects of shear and plastic deformation are significant, thus making the pore volume changes also significant^[1].

Flow properties, or permeability, are altered as an effect of changes in stress strain and compaction. Usually stress dependent porosity is identified while stress dependent permeability is mostly unaccounted for. This type of coupling is mostly present where pore volume changes are significant. It is also highlighted where compressibility is highly

governed by the fluid, for example gas reservoirs, where the gas accounts for most of the total compressibility of the porous media [1].

Porosity is the fundamental component for volume coupling. What will be presented now is the original iterative algorithm used to calculate porosity change. It constitutes several steps.

Step 1: Calculation of the porosity in the reservoir simulator based on pressure and temperature

$$\phi^* - \phi^n = \phi^{(i)} [C_p^{(i)}(p - p^0) - C_t^{(i)}(T - T')] + \Delta t(\Delta \phi_t^{(i)}) \quad [1] \dots\dots\dots (6)$$

Cp Ct and Δt(ΔΦt) are used from the previous iteration

Step 2: Get the new solution for the new iterate for P and T from the reservoir simulator, and insert them in the stress model, solving the stress equation to get the new iteration for $\Delta \sigma_{x,y,z}$ and $\Delta \epsilon_{x,y,z}$ [1]

Step 3: calculate the true porosity:

$$\phi^{(i+1)} = \phi^n + [C_b(1 - \phi^0) - C_s] \cdot [(p^{(i+1)} - p^n) - (\sigma_m^{(i+1)} - \sigma_m^n)] \quad [1] \dots\dots\dots (7)$$

Step 4: calculate the new iteration for C_p^{k+1} , C_t^{k+1} and $\Delta t(\Delta \phi_t^{k+1})$. Note that Cp and Ct coefficient are constant for linear elasticity [1]

Step 5: Calculate the new volumetric strain thus the new porosity [1]

$$\epsilon_v^{(i+1)} = (\epsilon_x + \epsilon_y + \epsilon_z)^{(i+1)} \quad [1] \dots\dots\dots (8)$$

$$\phi^{*(i+1)} = \phi^{*n} + \phi^{(i+1)} [1 - \epsilon_v^{(i+1)} - \epsilon_v^n] \quad [1] \dots\dots\dots (9)$$

Step 6: check the convergence of the solution by taking $p^{k+1} - p^k$, if not converged redo the same steps [1].

Permeability

When predicting permeability changes, one must always choose the right model that expresses it in terms of significantly measurable reservoir rock properties. The Kozeny-Carman relationship is the first to link permeability to rock properties. This very important relationship has been reworked by many other authors. There are many other equations based on the Kozeny-Carman relationship that can be used for different situations, in other words, different types of rocks or porous media constituents. There are models based on grain size, mineralogy, surface area, water saturation, pore dimension [10].

Two way coupling for permeability updating works in a way that automatically updates permeability due to compaction data that could be represented as strain or as updated

porosity depending on the method used. At every time step a new permeability has to be calculated, thus many equations have been derived. Three methods will be tested and exploited in order to better understand their effect on the presented reservoir cases [9].

Based on **Kozeny-Carman**

$$\frac{K}{k_0} = \frac{\Phi^3}{(1-\Phi)^2} \dots\dots\dots (10)$$

Based on the **Polynomial Law**

$$Mult = \frac{[\phi^n]_{timestep}}{[\phi^n]_{initial}} \dots\dots\dots (11)$$

$$k_{timestep} = k_{initial} \cdot Mult \dots\dots\dots (12)$$

Based on the **Intact Porosity Table**

The intact porosity table works by creating a function out of realistic numbers of permeability updating with respect to decrease in porosity obtained from realistic data that can be field data or lab data. When the function is created it is inserted into the two way coupling model, thus the model follows the function in order to update the permeability accordingly.

Chapter 3: Case Study Results and Comments

In this chapter, results for two separate cases obtained from one way coupling and different methods implemented in the two way coupling approach will be presented. For each case, field production data graphs will be presented including field gas in place, field gas production and field pressure rate. Moreover, coupling simulations will be presented starting with one way coupling, pictures simulating the rock displacement in the reservoir and at the surface will be displayed along with graphs showing the evolution of rock displacement during production time. On the other hand, two way coupling simulation data will also be presented, but this time for different two way coupling approaches using different equations and functions as discussed earlier. The resulting graphs will all be compared with the original production data of each reservoir respectively.

I-CASE 1

The reservoir is a closed system with no aquifer and a depletion drive production mechanism. The sandstone reservoir is a medium depth gas reservoir at 1504 meters, with 3000 meters lateral extension and a 75-meter maximum thickness. The formation above the reservoir could be consolidated or unconsolidated sand and sandstone and the base region under the reservoir is carbonate rock forming the source rock. The initial pressure of the reservoir 158,69 bar and has

an unconfined compressive strength of 33.9 bar. The reservoir has a homogeneous and isotropic permeability of 50 mD and a porosity of 21%.

A- Reservoir Production Data

The field has 4 production wells producing simultaneously. Consequently, the production data from these wells over the course of 9 years and five months will be used in order to get an overview about how the reservoir fluid flow and reservoir conditions react to production. Hence, a reservoir simulator was used in order to get cumulative gas production, reservoir pressure decline curve and recovery factor. The data was simulated in ECLIPSE and 2 scenarios were displayed; scenario 1 has production rate of each well as an input condition and scenario 2 has bottom hole pressure of each well as the input condition while setting an upper limit for cumulative gas production. This part of the case study is done in order to better understand the field we are dealing with and in order to choose the best operating conditions that suit our case study. The reservoir pressure conditions at the beginning of production and at the end of production, with its structure and well location was displayed using FLOVIZ. The Initial pressure conditions of the reservoir are displayed in figure 4.

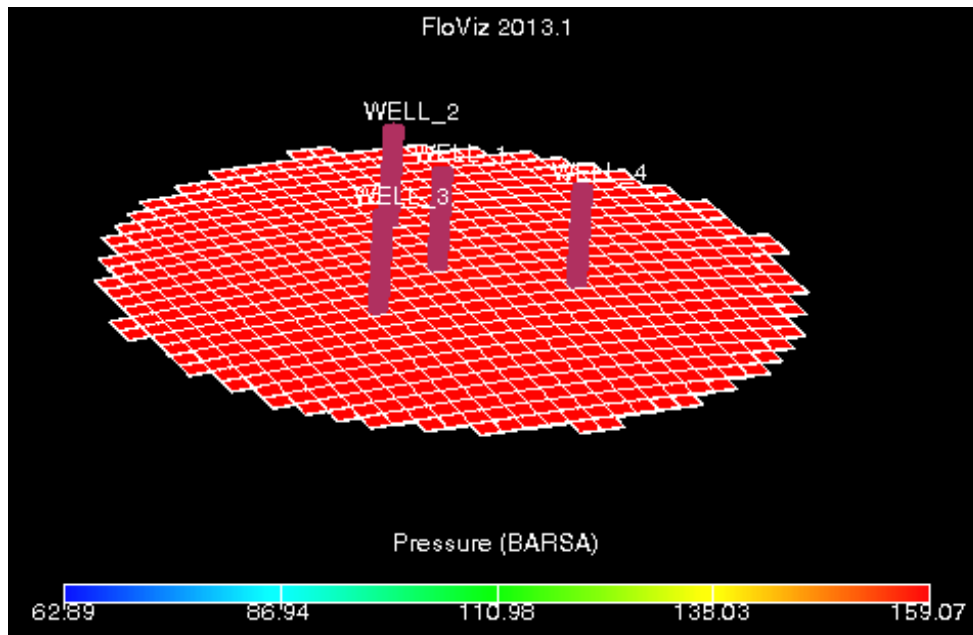


Figure 4 Reservoir Pressure Distribution before Production

i- Scenario 1

In this scenario, the well data were simulated on eclipse office based on production rate as an input condition for the WCONPROD key word in the eclipse data sheet, the results were the following:

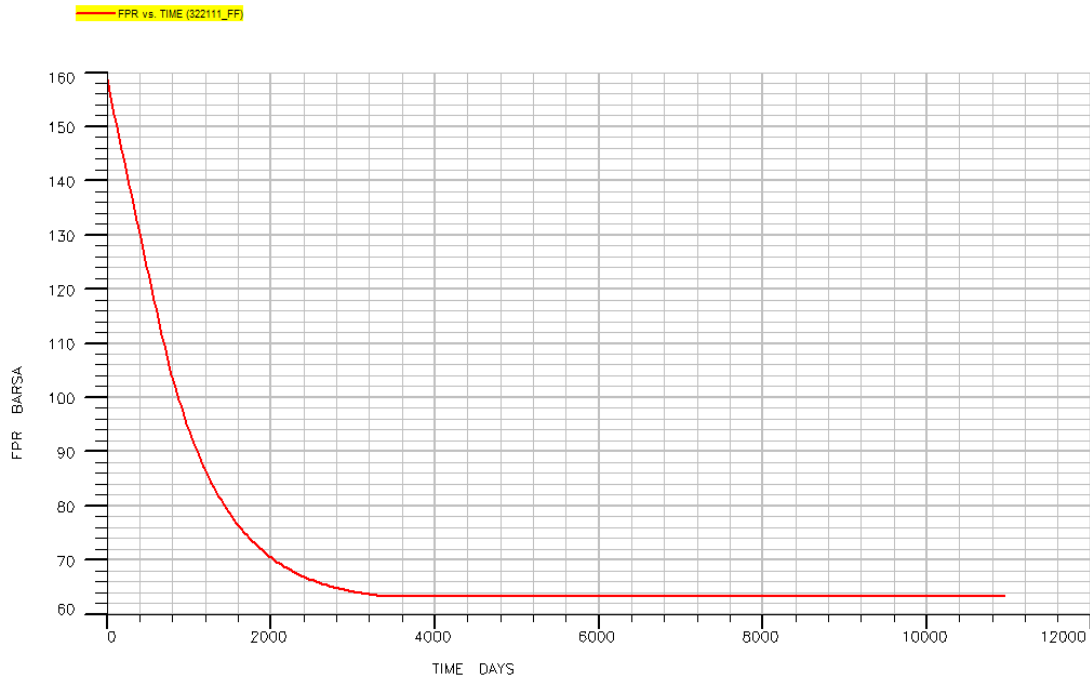


Figure 5 Pressure Decline Curve (case 1)

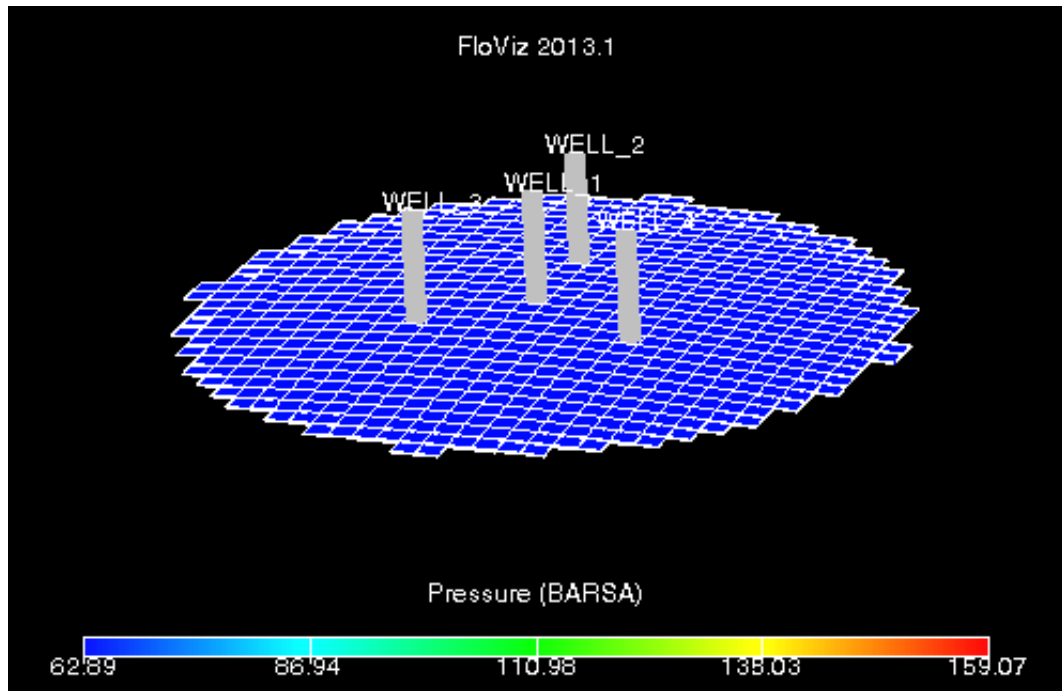


Figure 6 Reservoir Pressure Distribution at the end of production (case1)

The pressure decline curve in figure 5 shows the loss of pressure inside the reservoir which starts as 159.07 bars and reaches a value of 62.89 bars as it can be seen in the reservoir model simulated on Floviz in figure 6.

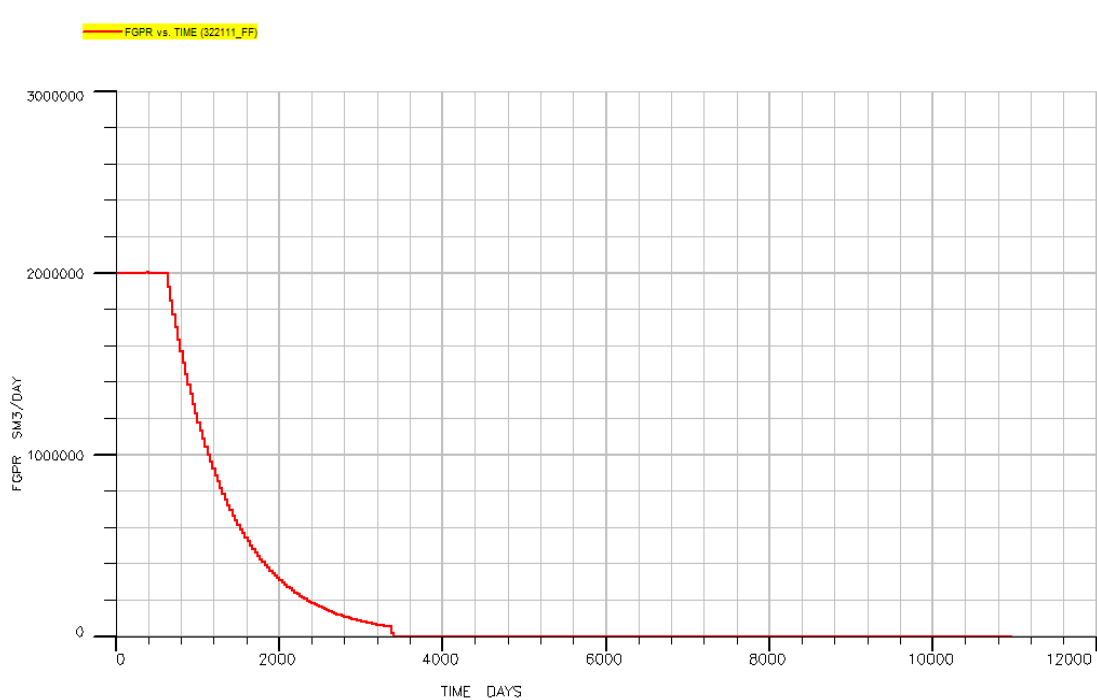


Figure 7 Cumulative Gas Production Rate (case 1)

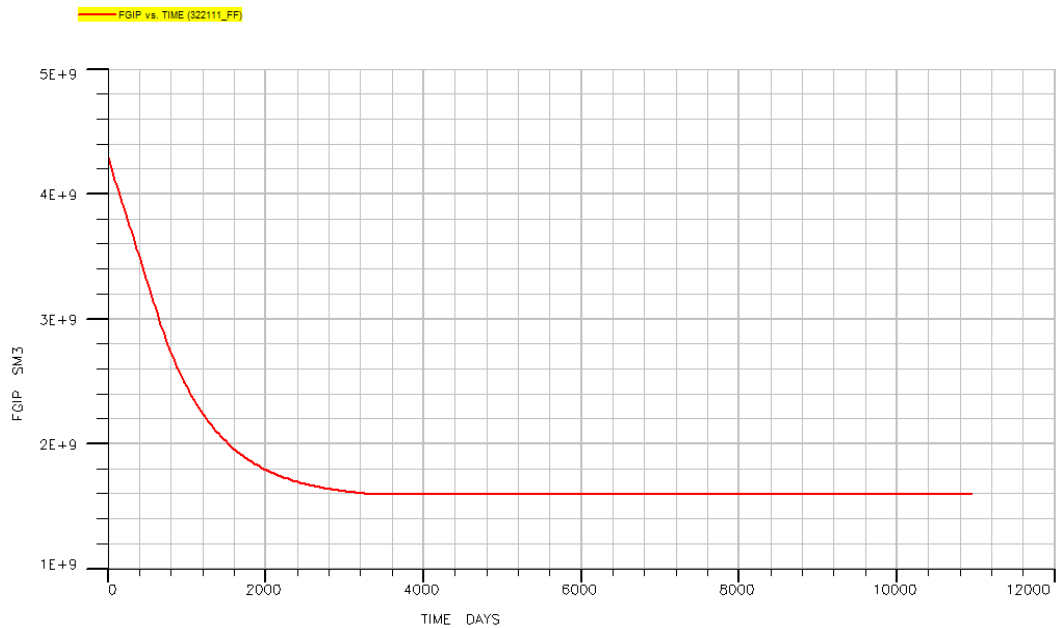


Figure 8 Gas Remaining in Place (case 1)

Figure 7 shows the cumulative production rate which started on January 1st 2016, at a rate of 2000000 sm³/day for all 4 wells combined. The production rate remained stable for about 1 year then it started gradually decreasing until it reached about 50000 sm³/day at the last few days of production and the wells were eventually shut down on May 1st 2025, after more than 9 years of production.

Figure 8 shows the remaining gas in place, and the recovery factor was calculated at the end of production using the results obtained. RF = 61.9%, which is relatively low for a depletion drive gas reservoir. The remaining gas in place trend is represented in the figure below. Due to the fact that the condition under the WCONPROD in the eclipse data sheet was used as gas rate and no condition was placed on bottom hole pressure, the rate decline started at 2000000 m³/day and declined fast until shut in, thus not exploiting the reservoir to the maximum and reaching such a low recovery factor.

ii-Scenario 2

In this scenario, the well data are simulated based on a minimum bottom hole pressure as an input condition at 5 bars for the WCONPROD key word in the eclipse data sheet and a cumulative production rate of $1.5 \cdot 10^6$ sm³/day was set. Our focus is to stress the system as much as possible in a realistic way, in order to accentuate the phenomena under analysis. The results were the following:

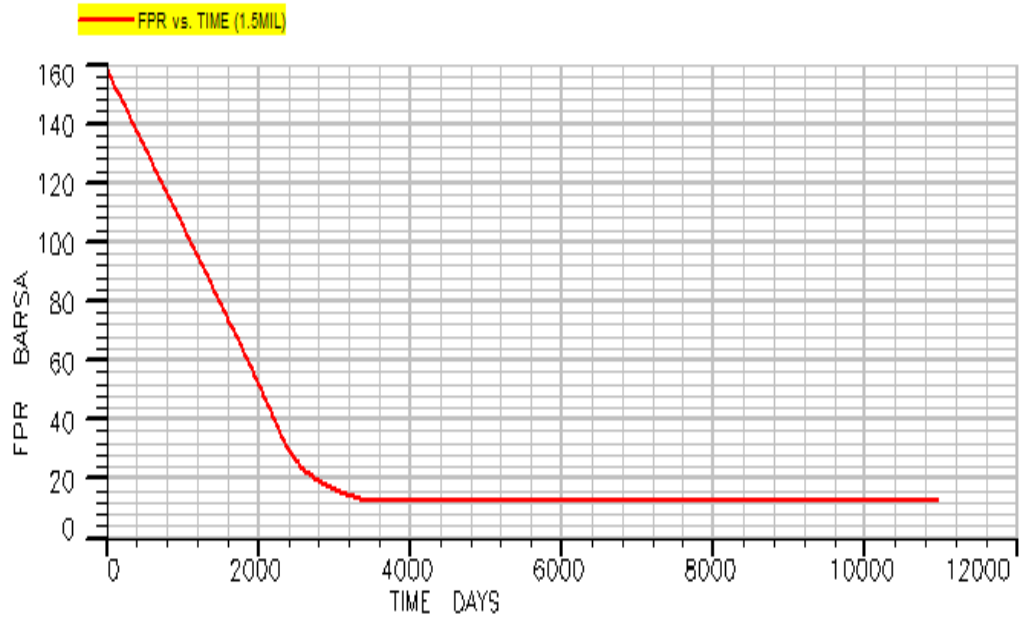


Figure 9 Pressure Decline Curve (case 2)

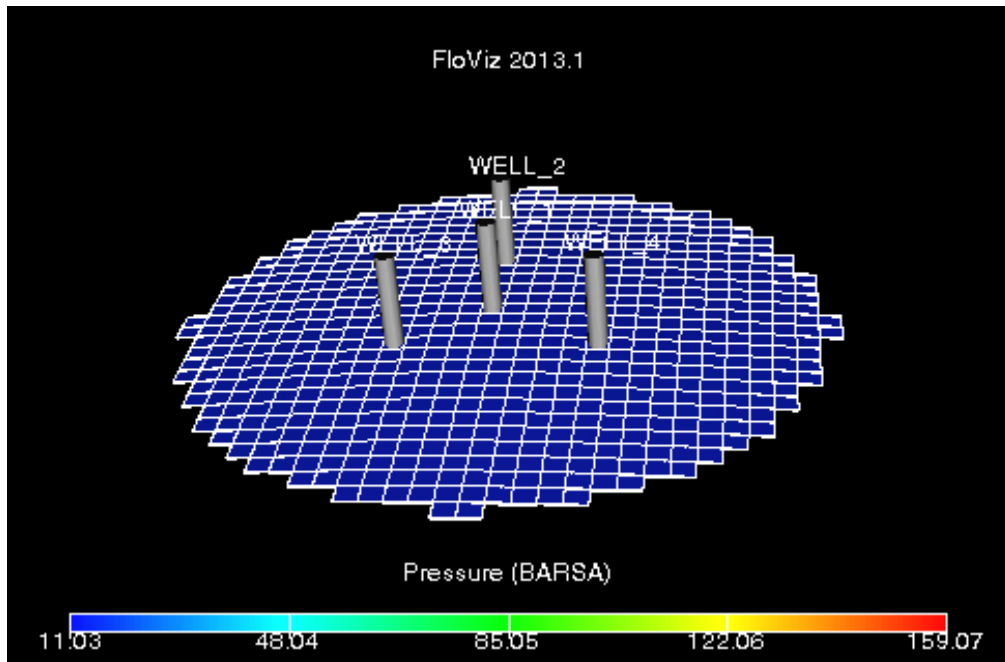


Figure 10 Reservoir Pressure Distribution at the end of production (case 2)

The pressure decline curve in figure 9 shows the loss of pressure inside the reservoir which starts as 159.07 bars and reaches a value of 11 bars as it can be seen in the reservoir model simulated on Floviz in figure 10.

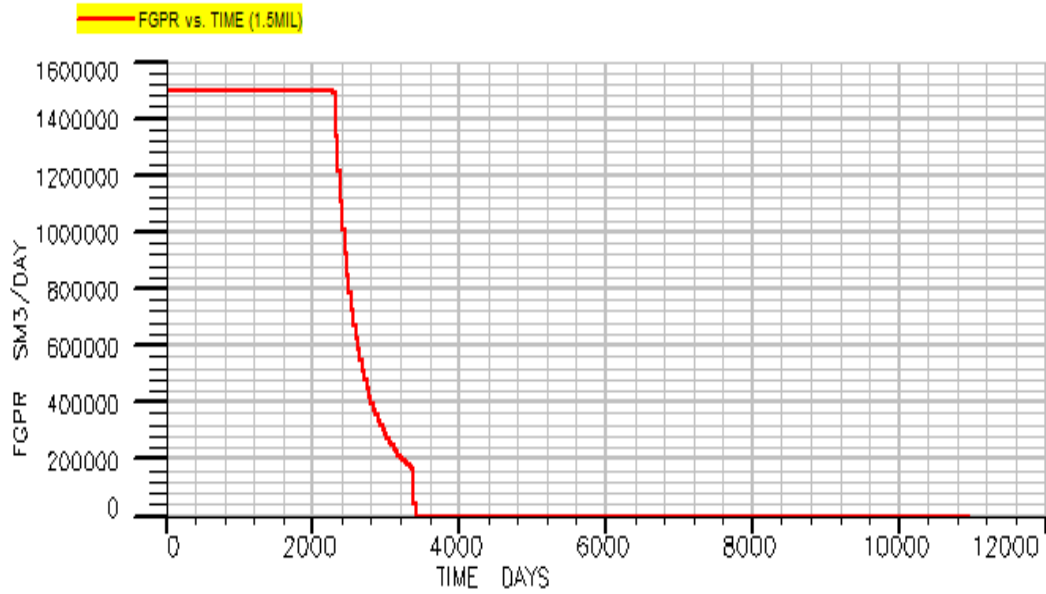


Figure 11 Cumulative Gas Production with respect to Time (scenario 2)

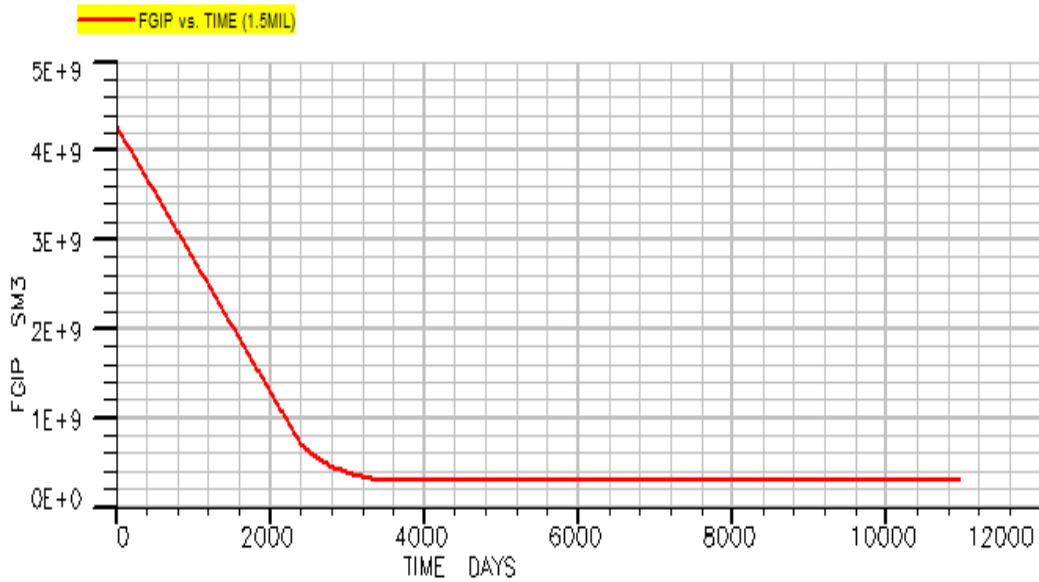


Figure 12 Remaining Gas in Place with respect to time (scenario 2)

Figure 11 shows the cumulative production rate that starts off at 1500000 sm³/day for all 4 wells combined. The production rate remained stable for most part of the production time at initial rate approximately until 6 years of production as can be seen in the plateau shown in figure 8. Due to the condition for the WCONPROD being 5 bars, the plateau was stable for a long time before it started to decrease and reached about 160000 sm³/day before the well was shut in after 9 years of production.

The remaining gas in place trend is represented in Figure 12. The initial gas in place is about $4.2 * 10^9 \text{ sm}^3$ and decreased to about $3 * 10^8 \text{ sm}^3$ at the end of production. The recovery factor, is about $\text{RF} = 92.5\%$. Now that the condition in the eclipse data sheet was set on bottom hole pressure (BHP) at 5 bars with a ceiling condition on production rate at $1500000 \text{ sm}^3/\text{day}$, the production rate can stay high for a longer time thus reaching a higher recovery factor.

Scenario 2 production data will be used as an input for the geomechanical simulations that will be performed for the upcoming parts of this study, since using scenario 2 we will be stressing the system to the maximum in order to get optimal coupling results.

B- One-way coupling

When producing hydrocarbons from a reservoir, the formation is subjected to compaction, which would lead to rock displacement in the reservoir and in the structure above the reservoir which would lead to subsidence at the surface. Subsidence could become a serious problem, since it could result in damages in the surface facilities and surrounding habitable areas. In this part of the case study, rock displacement was simulated using the production data for case 2 of the simulations presented in part A. Rock displacement data and pressure decline in the reservoir are demonstrated using VISAGE through PETREL.

i-Reservoir Geomechanics Simulation Data

Production of the gas from the reservoir causes reduction in pore pressure, which eventually will cause compaction of the reservoir rock. This part is crucial in our study since it is the basis for the second part of the case study which is assessing how the fluid flow properties are affected by rock compaction by applying 2 way coupling. Reservoir vertical displacement along with pressure decline are presented in the graphs and figures below.

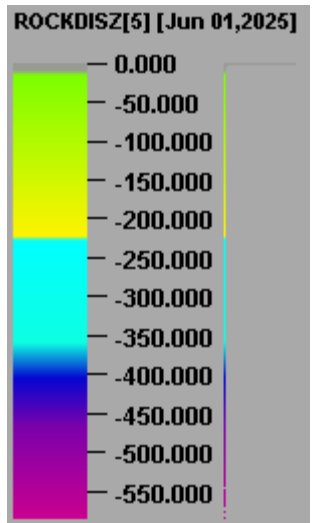


Figure 13 Legend showing rock displacement intensity in millimeters for figures 14 17 and 18

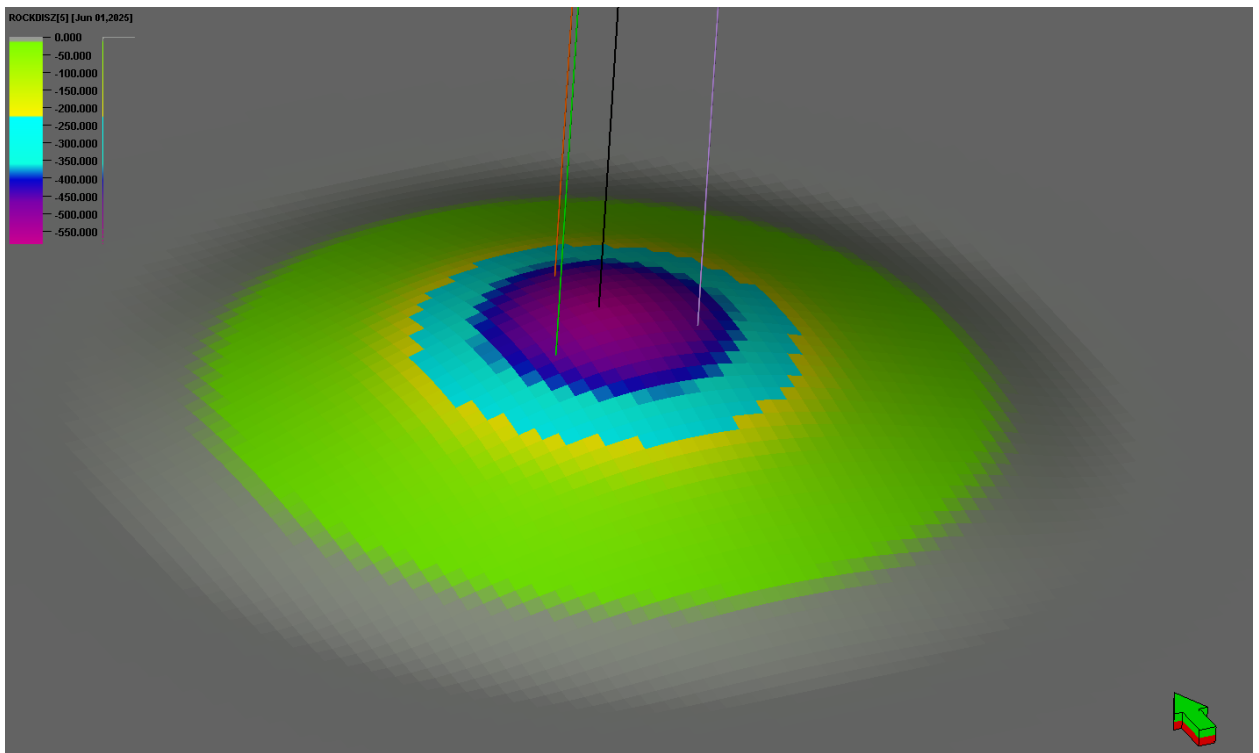


Figure 14 Rock Vertical Displacement in the Reservoir at the end of production in millimeters

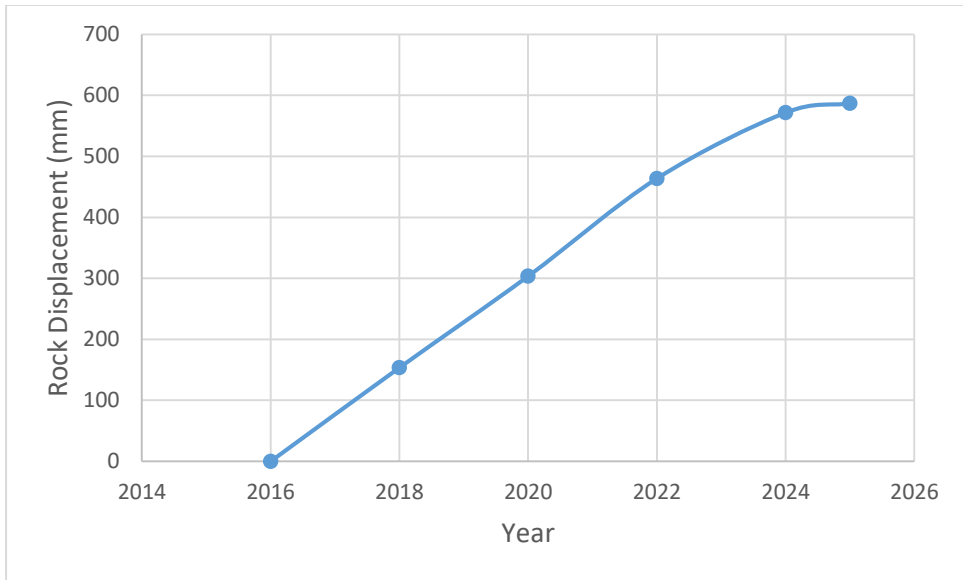


Figure 15 Rock Vertical Displacement in the reservoir as a function of Time

Rock displacement is shown in 3D in figure 14, gray being no or little displacement up until 1cm (10 mm) of displacement. The dark violet color is the highest level of displacement, ranging between 500 and 600 mm of displacement. Rock displacement started to increase gradually from the beginning of production until it reached about 568 mm of rock displacement as it can be seen in figure 15. This value was chosen from the cell in the grid experiencing the highest compaction intensity at each timestep.

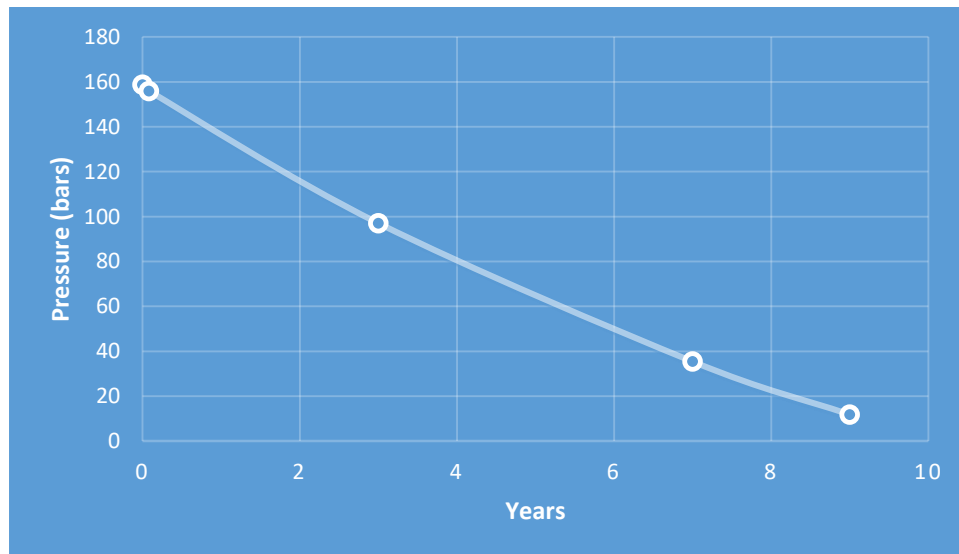


Figure 16 Pressure Decline Curve

The pressure decline curve seen in Figure 16 shows the pressure drop in the reservoir due to production. As it can be seen, one can relate pressure decline to rock displacement knowing that as pressure drop increases, rock compaction also increases.

ii-subsidence analysis

In cases where the formation is loose or unconsolidated, similar to the structure that was studied and presented in this paper, rock compaction and displacements that take place in the reservoir will naturally be reflected on the surface in the form of subsidence. Results of rock displacement seen in figures “12” “13” and “14” eventually resulted in the subsidence results simulated.

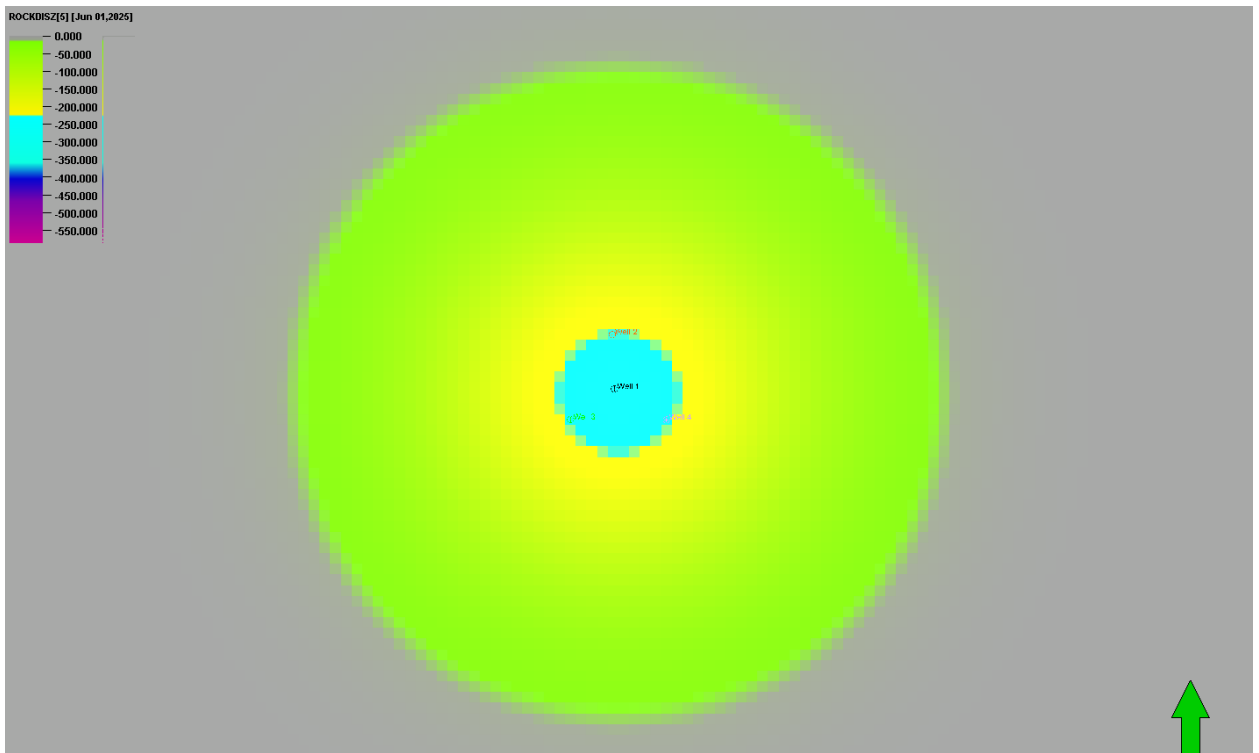


Figure 17 Rock vertical Displacement on the Surface

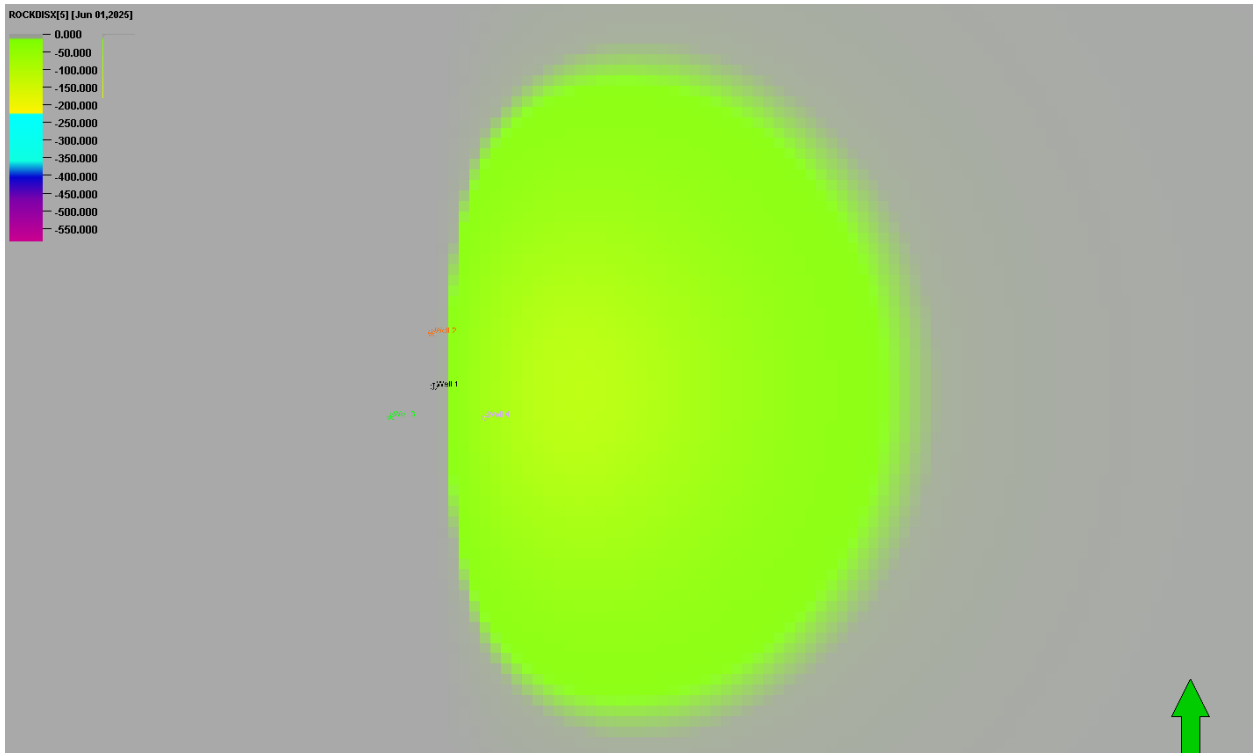


Figure 18 Surface Vertical Rock Displacement

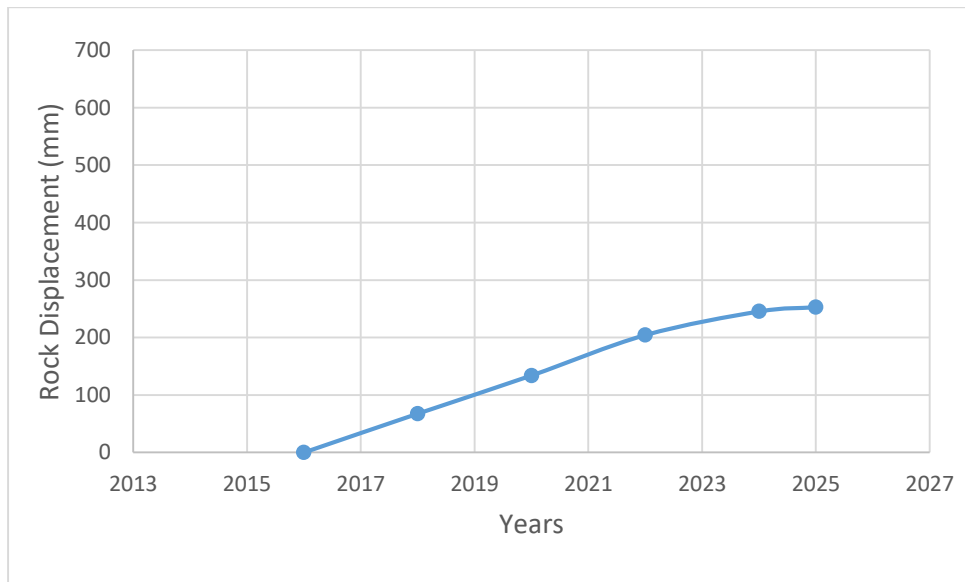


Figure 19 Rock Vertical Displacement at the Surface with respect to Time

Rock displacement in the reservoir can be easily reflected in shallow reservoirs with weak or unconsolidated formations like sandstone. As in figure 14 and 15, rock displacement at the surface is represented in figures 18 and 19. Figure 18 follows the same legend (figure 13) as figure 12. The rock displacement starts to increase slowly until it reaches 252.85 mm.

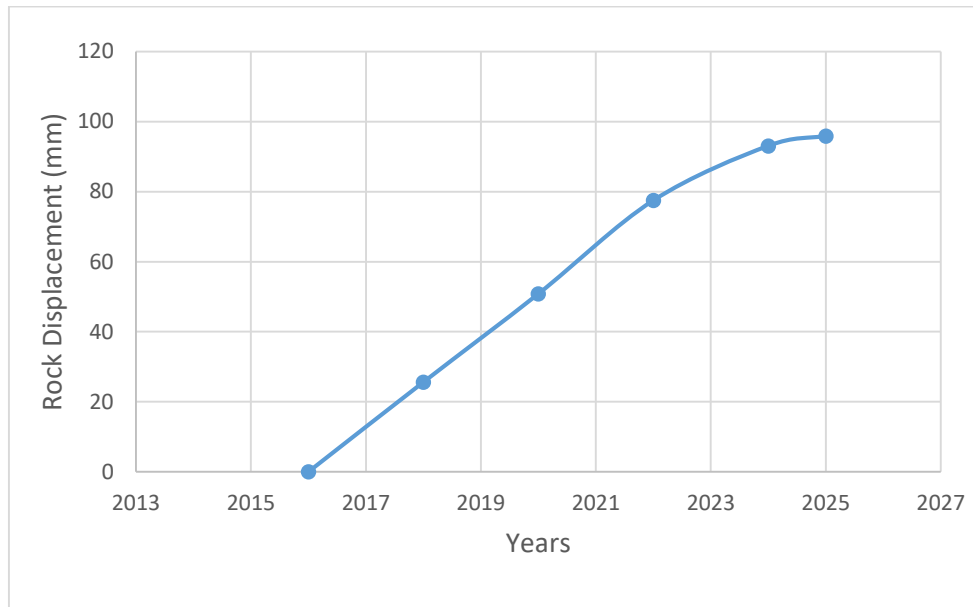


Figure 20 Rock Lateral Displacement at the Surface with respect to Time

The lateral rock displacement in the Lateral direction were also recorded as it can be seen in figure 20, that shows a rock displacement of 96 mm in every direction. Lateral displacement is also important to record since it causes cracks which could allow gas migrations to the surface.

Table 1 Medium Depth Reservoir Rock Displacement vs Surface Subsidence vs Subsidence Impact Radius

Time Step	Reservoir Maximum Rock Displacement (mm)	Surface Subsidence (mm)	Subsidence Radius (m)
2016	0	0	0
2018	154	68	2292
2020	304	134	2695
2022	464	204	2844
2024	554	245	3102
2025	568	253	3131

Table 1 shows the difference in rock displacement between reservoir rock and surface subsidence. Reservoir rock displacement and surface subsidence are only equal in the case of infinite lateral dimensions of the reservoir. The magnitude of the difference between reservoir compaction and surface subsidence primarily depends on; reservoir depth, lateral extent of the reservoir and characteristics of the overlying rock.

In this case study, surface subsidence is about 253 mm, less than half the reservoir rock displacement (about 45%) which is about 568 mm after about 9 years of production as shown in figures 15 and 19 respectively.

Table 1 also shows the surface subsidence impact radius which reaches about 3131 meters. This radius is very large and will affect an area of 30 Km² (keeping in mind that the intensity varies widely as the radius enlarges as it can be seen in figure 17), consequently this might cause damages to all surface equipment including gas pipes and well heads which would be disastrous and can cost lives and money.

C- Two Way Coupling

This case, as stated previously is a typical case of a reservoir in the Adriatic sea and the point of two way coupling here is to try and understand the degree to which the compaction effects due to production can affect reservoir petrophysical properties and might eventually affect pressure drop and production rate in the reservoir leading to higher remaining hydrocarbons in place, consequently lower recovery factors than expected in a fixed production time. Therefore, it is important in cases like these to take into account the changes in permeability due to strain and porosity decrease and to monitor its effect on pressure in the reservoir, production data and recovery factor. This is done by running a reservoir simulation case on VISAGE reservoir geomechanics which generates a new permeability at each time step selected based on the any chosen permeability update function that could be one of the of the functions stated part E of chapter 2.

Visage works in one of two ways while running a two way coupling simulation, the first being using existing generated strains to update porosity and then update permeability accordingly based on the equation or method selected.

Visage updates Porosity in the following way ^[12]:

$$\Delta\phi = \alpha * \epsilon_v \dots\dots\dots (13)$$

$$\phi = \phi_{initial} + \Delta\phi \dots\dots\dots (14)$$

Then, permeability is updated depending on the chosen equation or method that needs to be applied. This could be Kozeny-Carman, Polynomial law with a porosity exponent of 10 in order to stress the system as much as we can and the intact porosity function which is derived from lab data. As discussed in chapter 2, the permeability curves displayed in the upcoming parts are permeability values chosen for a single cell in our reservoir which experiences the highest degree of permeability reduction.

Kozeny-Carman

Results using this equation are displayed below

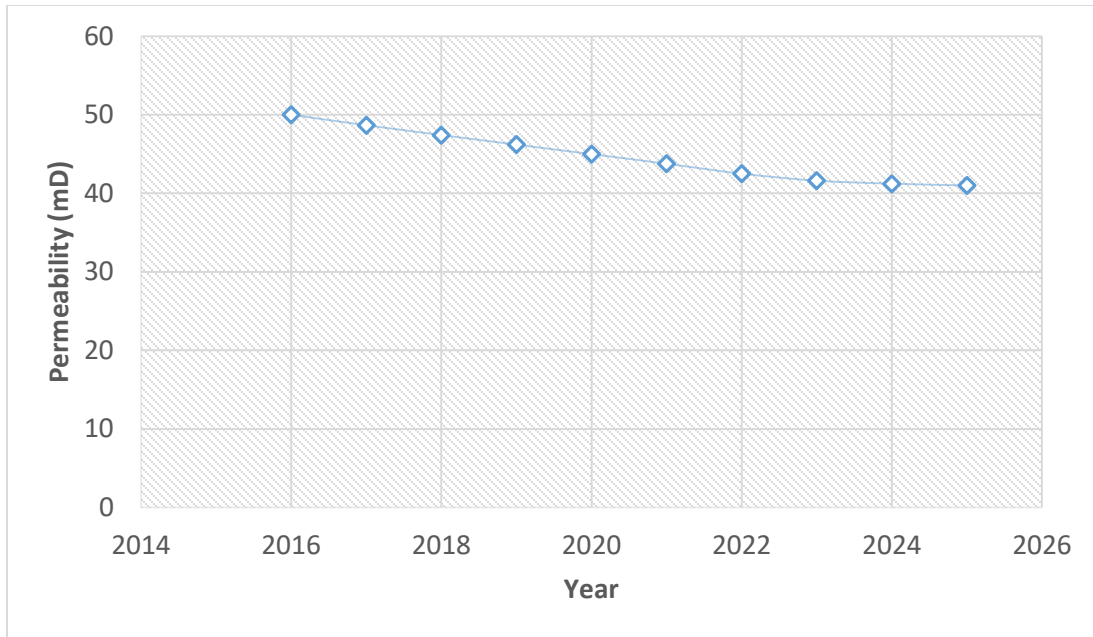


Figure 21 Permeability Decline Kozeny-Carman

Using equation 10, Visage calculated the decline in permeability using the changes in porosity due to strain to update permeability. Figure 21 shows the decrease in permeability from the start of production until the end. From an initial value of 50 mD, a minimum value of 40.987 mD is reached.

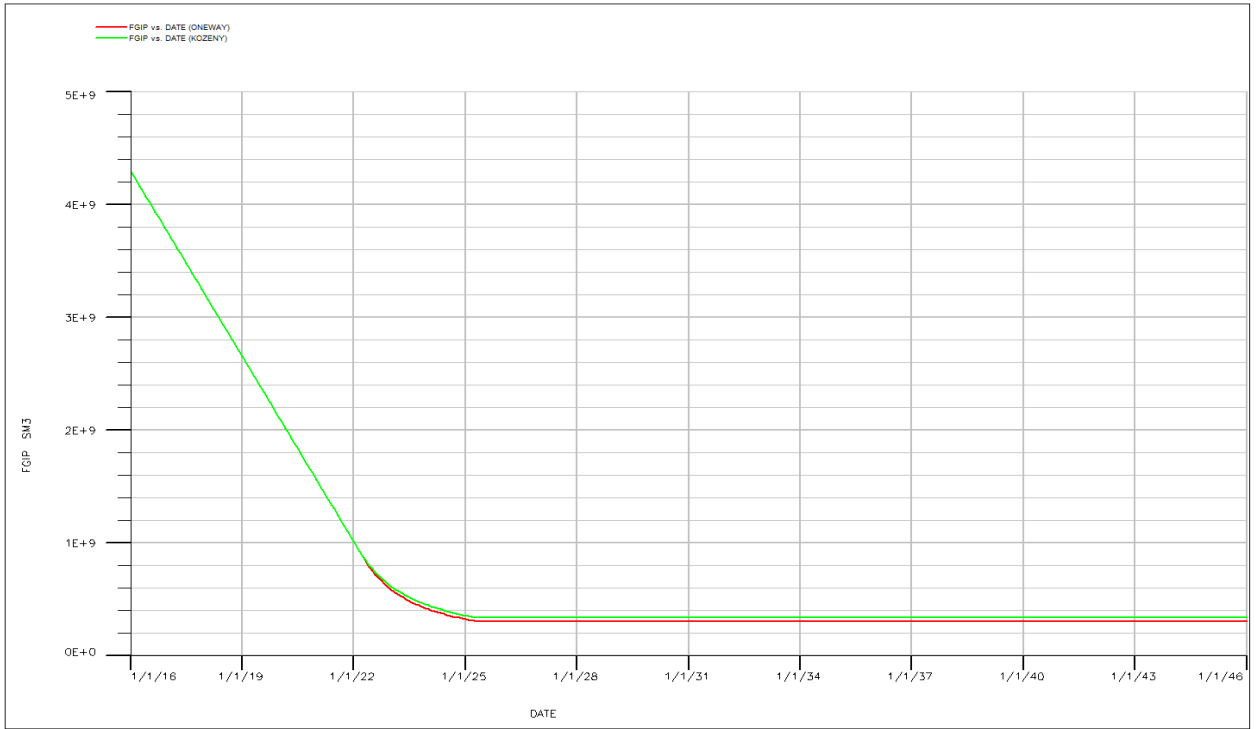


Figure 22 Gas in Place with respect to time One Way (Red) vs Kozeny-Carman (Green)

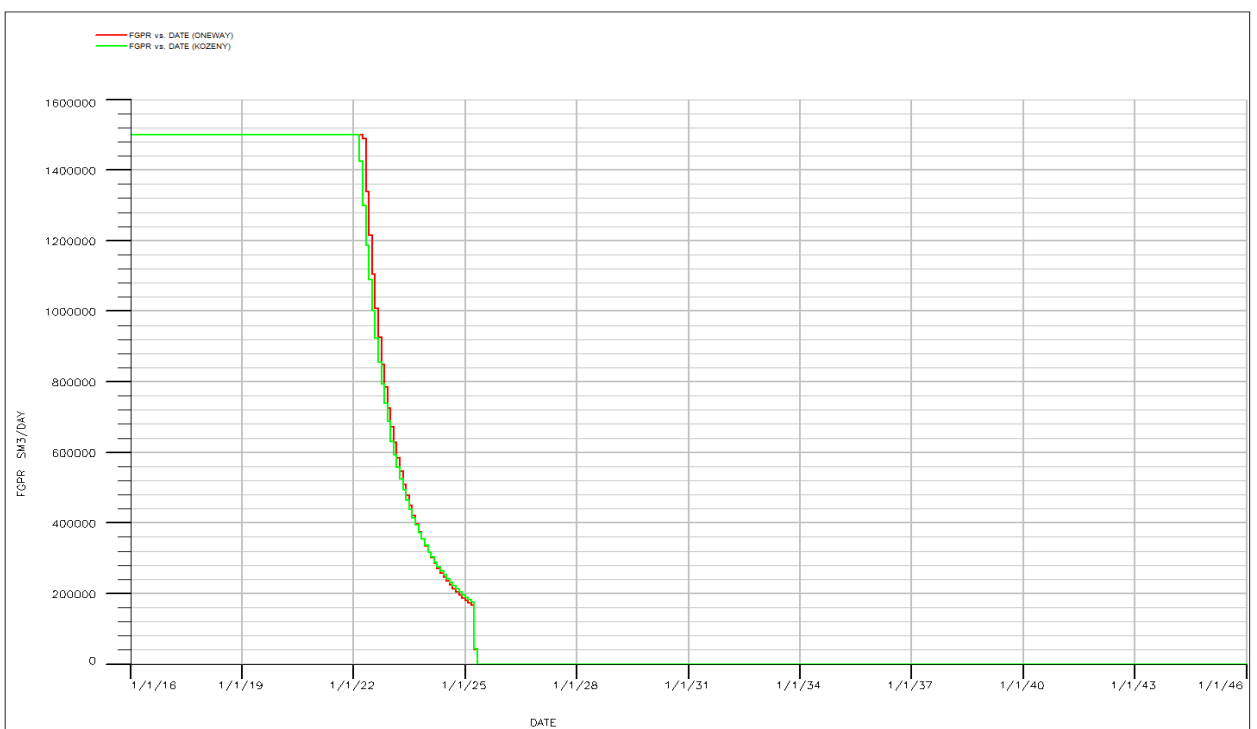


Figure 23 Cumulative Gas Production with respect to Time One Way (Red) vs Kozeny-Carman (Green)

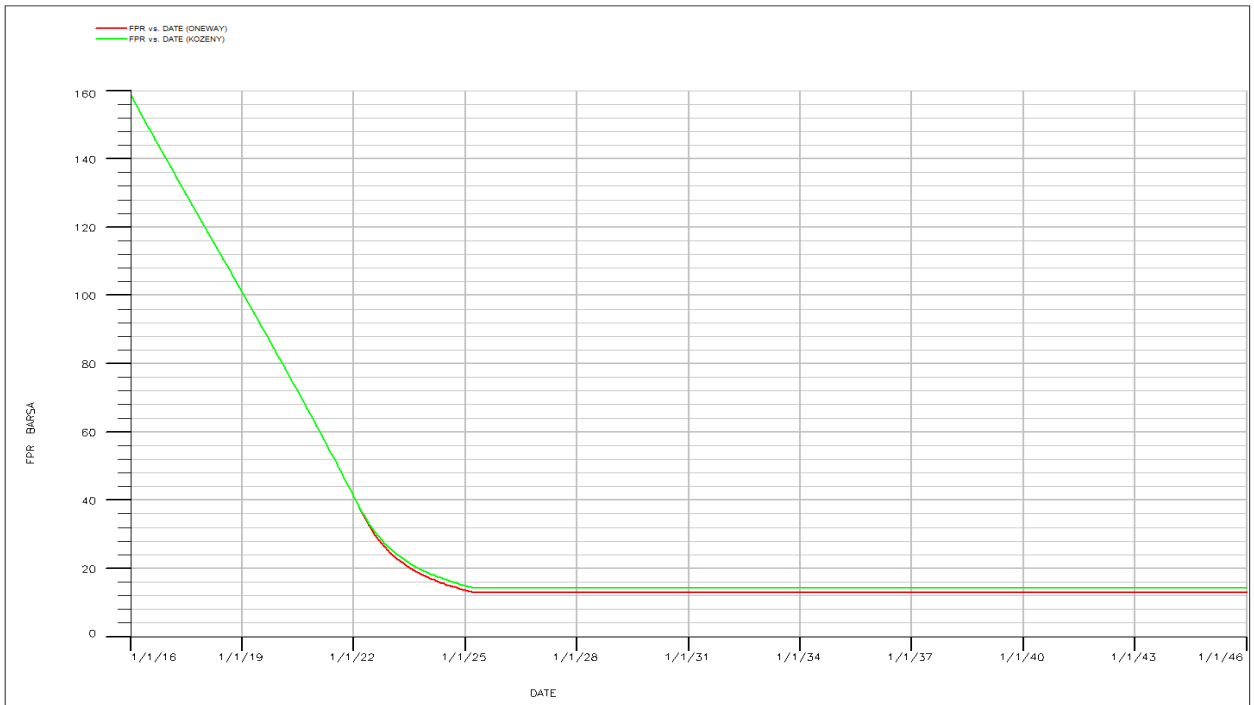


Figure 24 Pressure Decline Curve One Way (Red) vs Kozeny-Carman (Green)

It can be seen that there is no significant change in reservoir production data between the one way coupling curve and the Kozeny-Carman curve. The permeability decrease in the two way coupling approach is not significant enough to cause abrupt changes in the pressure decline curve, gas production rate and consequently recovery factor. Since there was no significant change in the production data between one way coupling and the Kozeny-Carman two way coupling method, rock displacement was also barely affected.

Polynomial Law (equation)

Results using this equation are displayed below

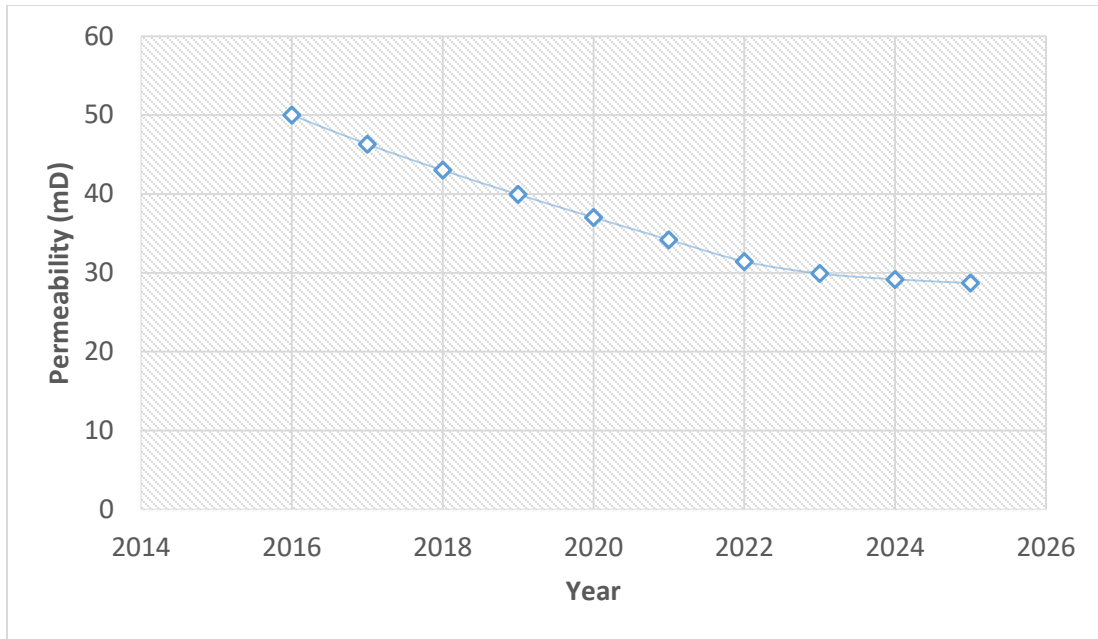


Figure 25 Permeability Decline Curve Polynomial Law

Using equation 11 with a porosity exponent of 10 which is an extreme case, visage calculated the decline in permeability using the changes in porosity due to strain. Figure 25 shows the decrease in permeability from the start of production until the end, and it can be clearly seen that the permeability decrease using the polynomial law is significantly more aggressive than when using Kozeny-Carman. A minimum value of 28.688 mD is reached.

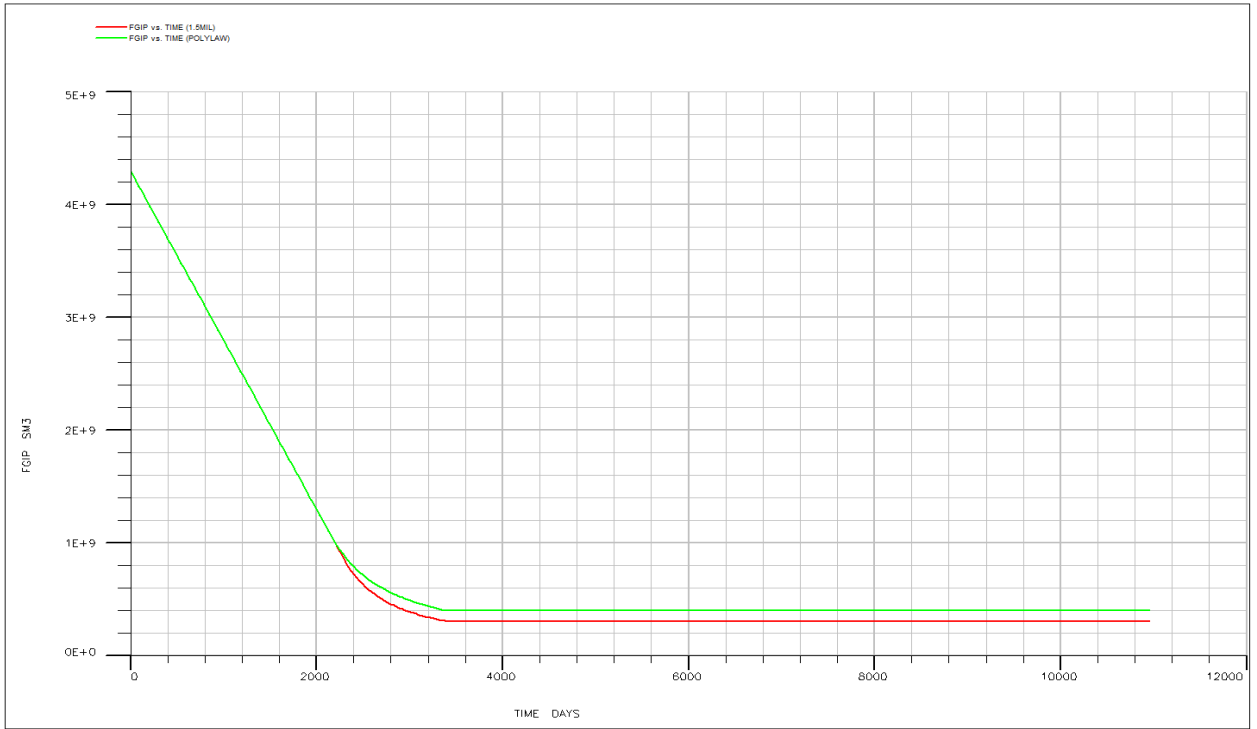


Figure 26 Gas in Place with respect to time One Way (Red) Polynomial Law (Green)

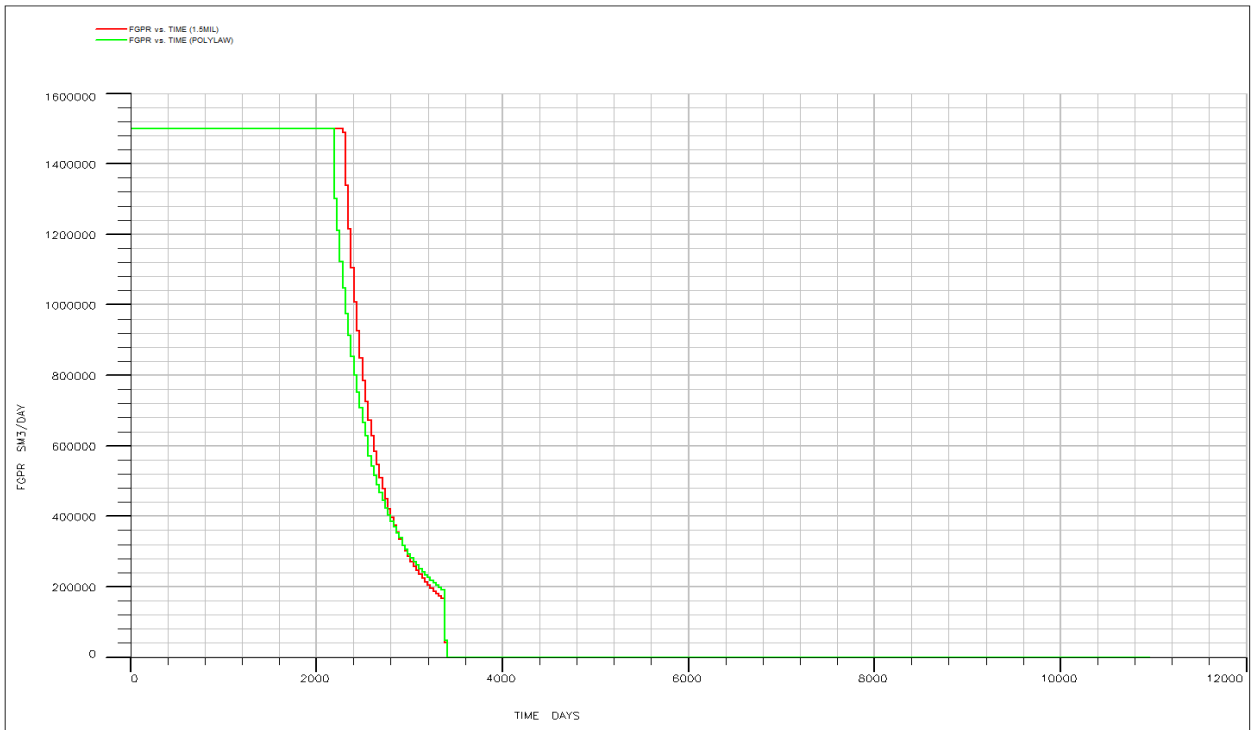


Figure 27 Cumulative Gas Production with respect to Time One Way (Red) Polynomial Law (Green)

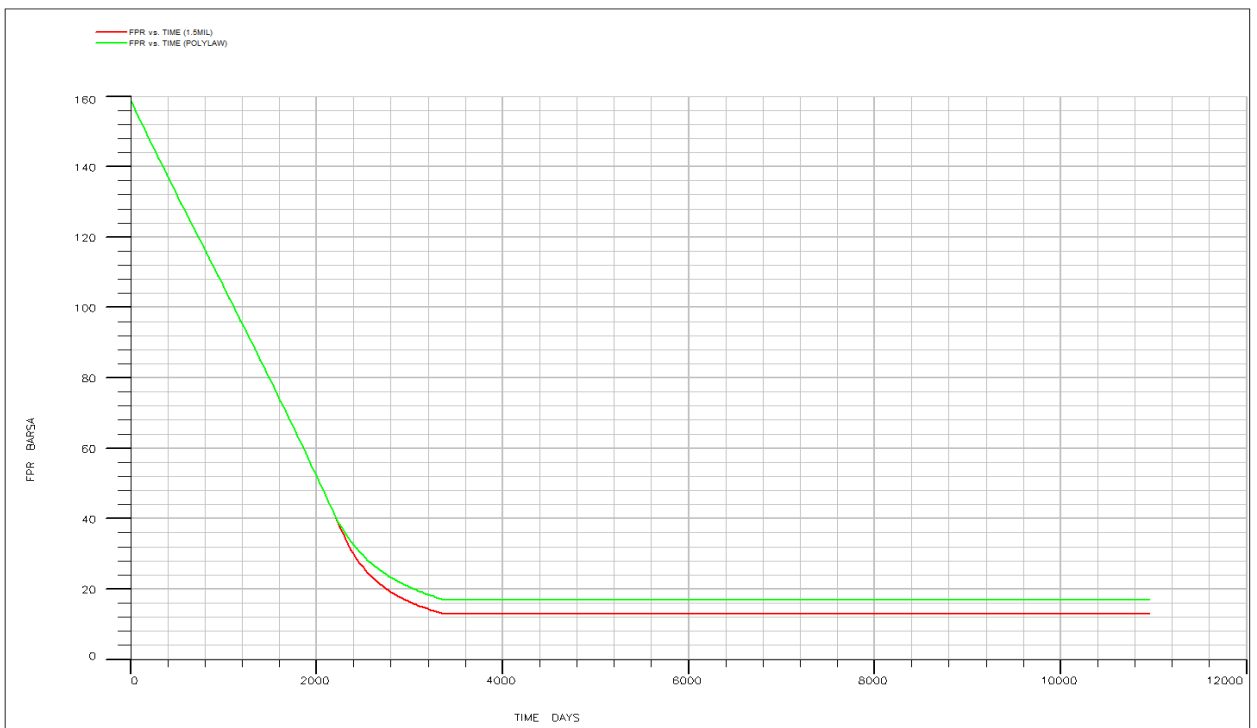


Figure 28 Pressure Decline Curve One Way (Red) Polynomial Law (Green)

Production data wise, even if the decrease in permeability is more significant than the Kozeny-Carman method, it can also be noticed that there is no significant difference between the one way coupling approach and the Polynomial law two way coupling approach. The 20 mD decrease in permeability, which only slightly hinders pressure decline, is not high enough to cause an abrupt change in production data as it can be seen in figures 26,27. Pressure in the reservoir at the end of production in the Kozeny-Carman case is slightly higher than the one way coupling case as it can be seen in figure 28. The pressure value is approximately 4 bars higher at about 16 bars in the Kozeny-Carman simulation compared to a previous 12 bars in the one way coupling simulation.

Intact Porosity Table (equation)

Intact Porosity Table method, is a method found in the visage geomechanics simulator where one can insert allows to use data from laboratory analysis. In this section, the data presented in figure 29, is data retrieved from the paper “Permeability evolution during triaxial compaction of an anisotropic porous sandstone” [13] where triaxial compaction of porous sandstone at different confining pressures is performed and analyzed. This data will be used as an input to the intact porosity table function that will be used to simulate porosity and permeability changes in our system.

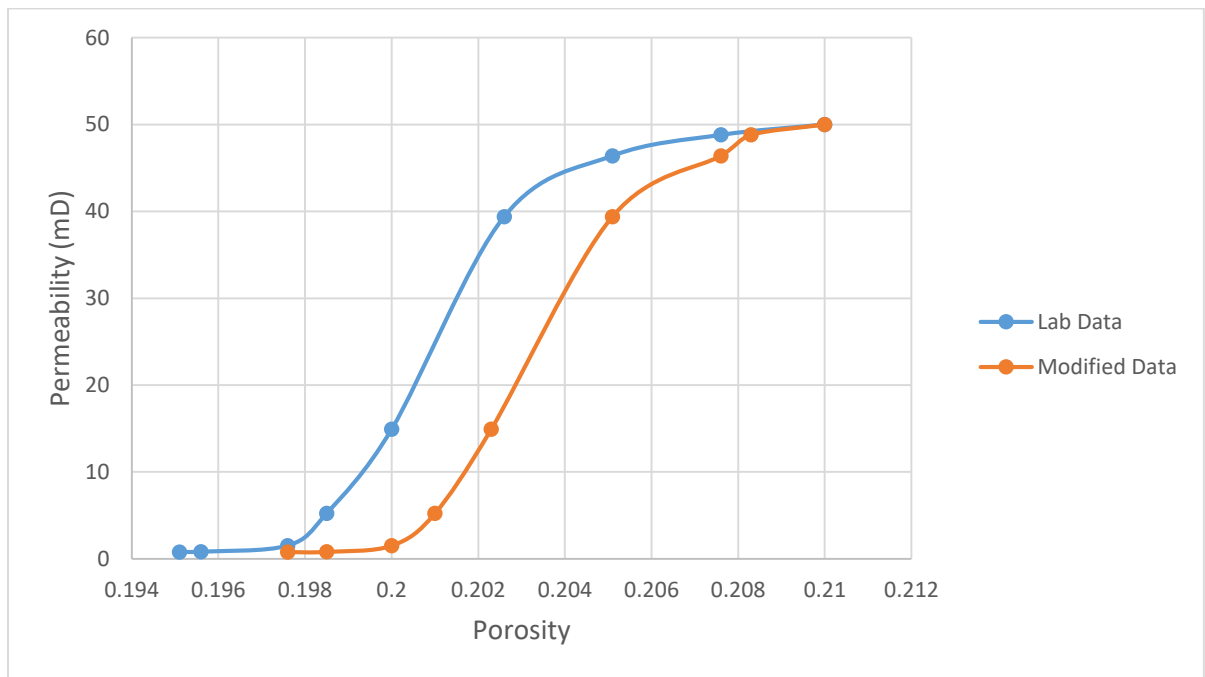


Figure 29 Lab Data; Normalized and Modified

Since it was not possible to find triaxial data for sandstone with the same permeability, same porosity and the same confining pressure, it was necessary to settle to one or two similar attributes and normalize based on these attributes. Results using this data are

displayed below. It is important to note that the lab data from the paper’s initial permeability is normalized to our 50 mD original permeability case and the orange curve labeled “Modified Data” is the exaggerated case based on the normalized data.

The reason behind the use of exaggerated data is to apply extreme changes in permeability in order to get appreciable coupling results. The results obtained from this exaggerated case are useful for cases that might have similar permeability and porosity changes with increased compaction.

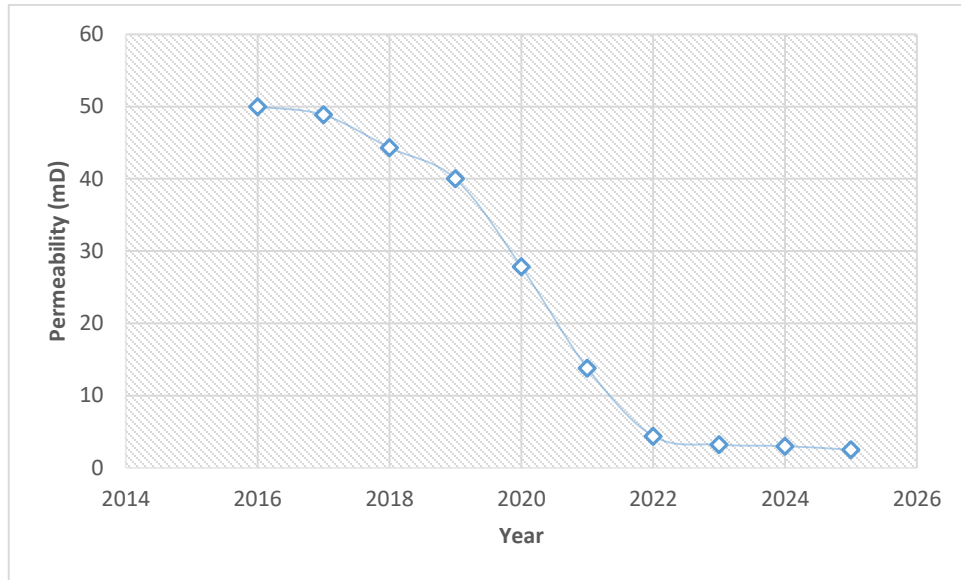


Figure 30 Permeability Decline Intact Porosity Table

Using the “Modidied Data” curve seen in figure 29, Visage updated the permeability based on the porosity changes in our system, and calculated the permeability in each timestep. This simulation resulted in a change of one order of magnitude in permeability to about 3 mD as it can be seen in figure 30. It is important to know that this data is exaggerated thus it produces unique results as discussed before.

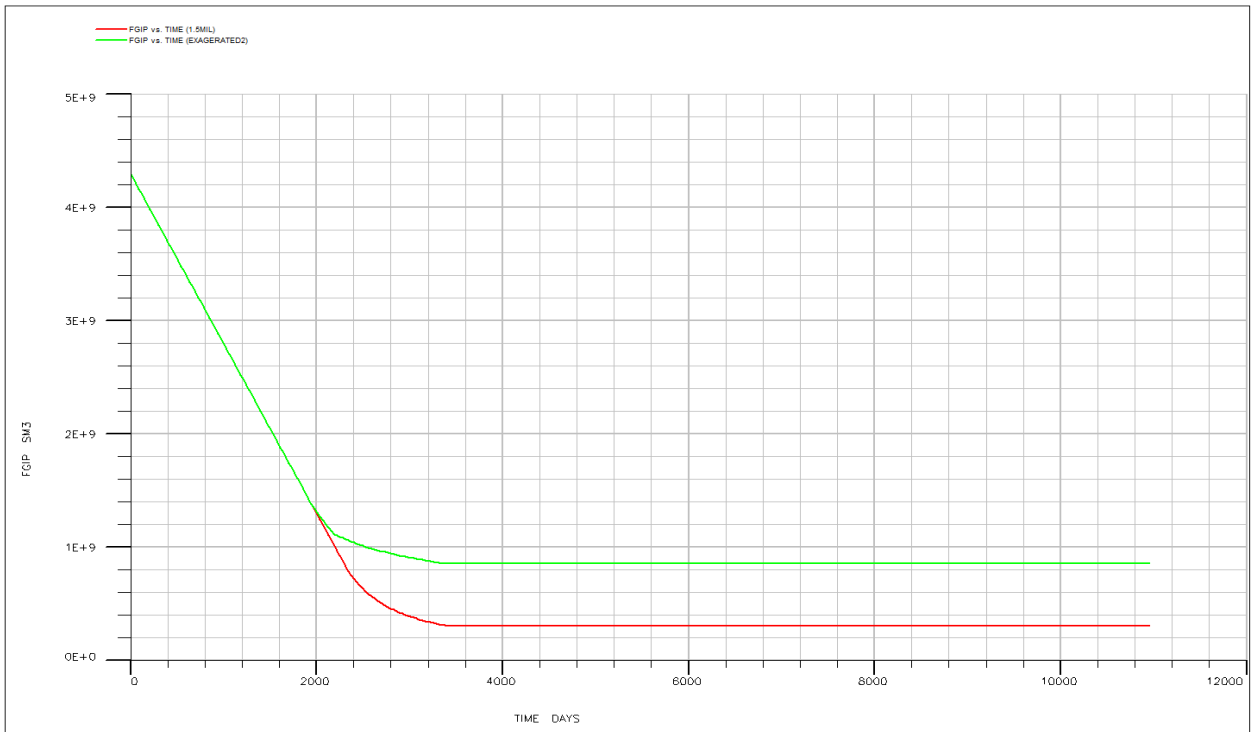


Figure 31 Gas in Place with respect to time One Way (Red) vs Intact Porosity (Green)

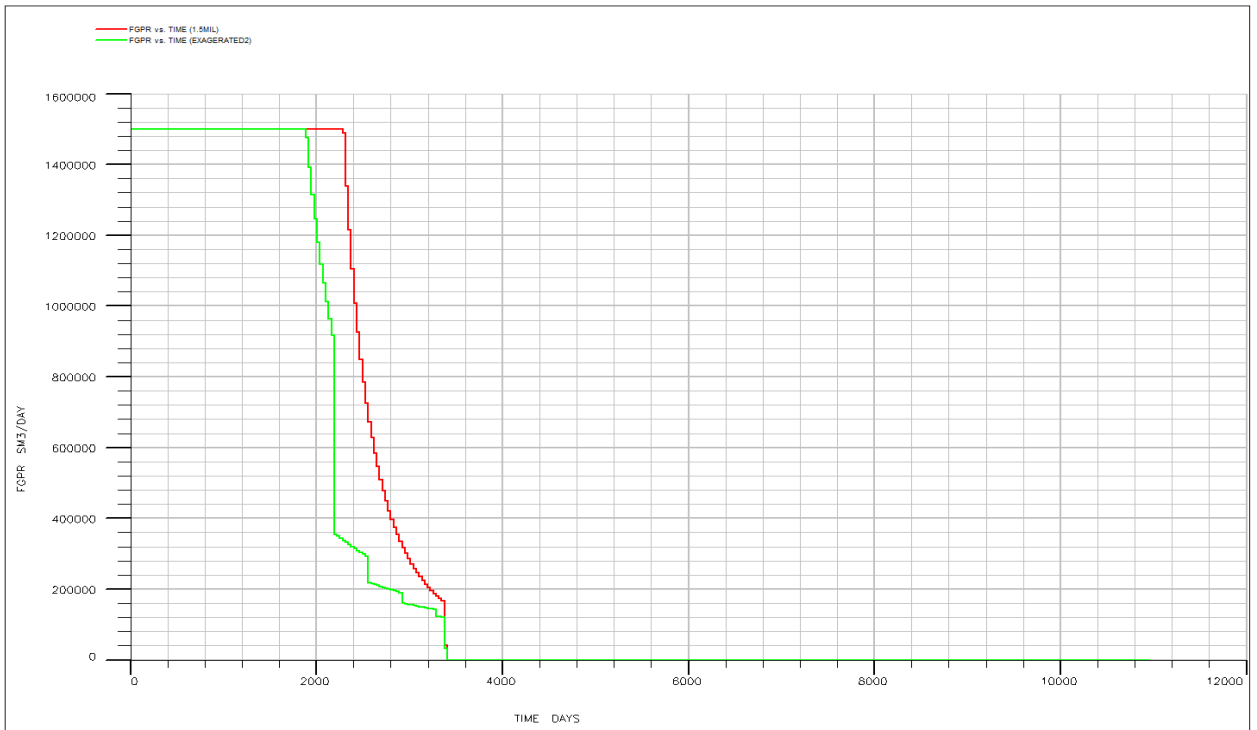


Figure 32 Cumulative Gas Production with respect to Time One Way (Red) vs Intact Porosity (Green)

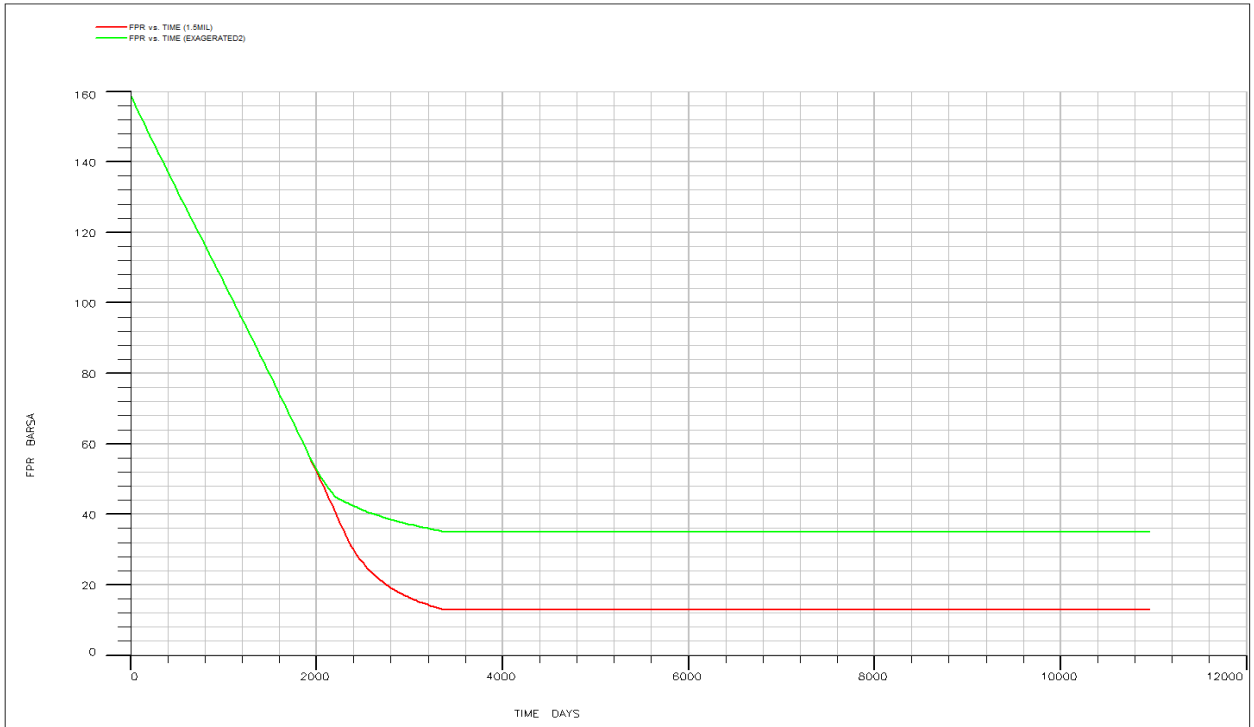


Figure 33 Pressure Decline Curve One Way (Red) vs Intact Porosity (Green)

Figures 31, 32 and 33 show the significant change in production data due to an abrupt decline in permeability due to strain caused by production. The significant difference in remaining gas in place between the one way coupling method and the intact porosity table method, reflects the strong impact reservoir compaction could have on well production due to the decrease in permeability. In figure 32, the huge discrepancy between well cumulative production curves in both cases is quite significant and most definitely affects all other aspects of production data. In figure 31, we can see that the remaining gas in place increased to about $8.5 * E^8 sm^3$, which decrease recover factor to about 80.9%. The discrepancy in pressure decline is also very significant in this case as it can be seen in figure 33, where the end pressure of the reservoir is at about 35 bars compared to a 12 bars in the one way coupling simulation. In this case, the abrupt decrease in permeability severely affected production data which led to a very significant decrease in recovery factor from 92.5% to 80.9%.

II-Case 2

In this case, the reservoir was shifted up to 300 meters in order to study the results the same way that was done for the Reservoir of case 1 and then compare the two cases where possible. This reservoir is a shallow reservoir at 300 meters depth with lateral extension of 3000 meters and depth of about 75 meters, just like case 1. The reservoir also has the same petrophysical properties as the reservoir of case 1 and it most likely has a poorly consolidated to unconsolidated sandstone formation due to its shallow depth, having a young modulus of 0.2 and

a Poisson's ratio of 0.3. The reservoir initial pressure is 40 bars and it has an unconfined compressive strength of 8.2 bar. The reservoir production data along with one way and two way simulation results are presented below.

A- Reservoir Production Data

The data was simulated in ECLIPSE and only one scenario is simulated in that case. The scenario is the same as reservoir 1's scenario 2 with bottom hole pressure of each well as the input condition while setting an upper limit for cumulative gas production at 1500000 sm³/day. This data will be presented along with coupling data in part C. The reservoir pressure conditions at the beginning of production and at the end of production, with its structure and well location was displayed using FLOVIZ in figure 34.

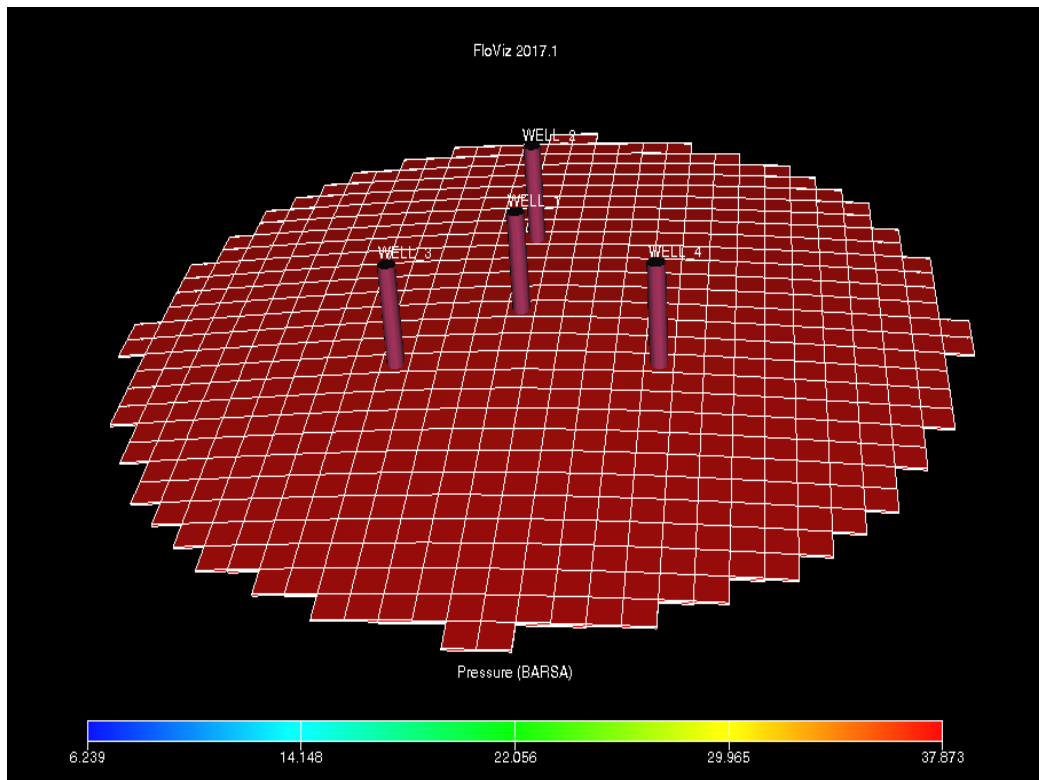


Figure 34 Pressure Distribution

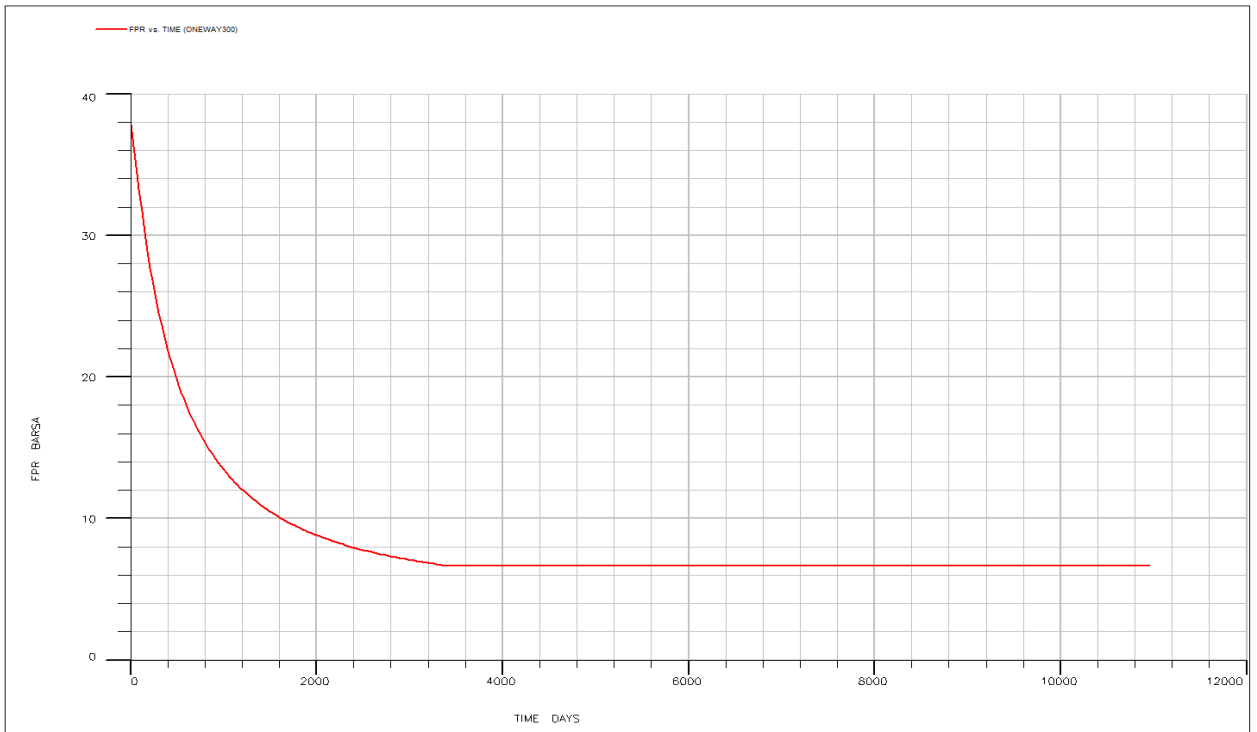


Figure 35 Pressure Decline Curve One Way Coupling

Figure 35 shows the pressure behavior in our reservoir which has an initial pressure of 40 bars and declines gradually during production and reaches about 6 bars at the end of production.

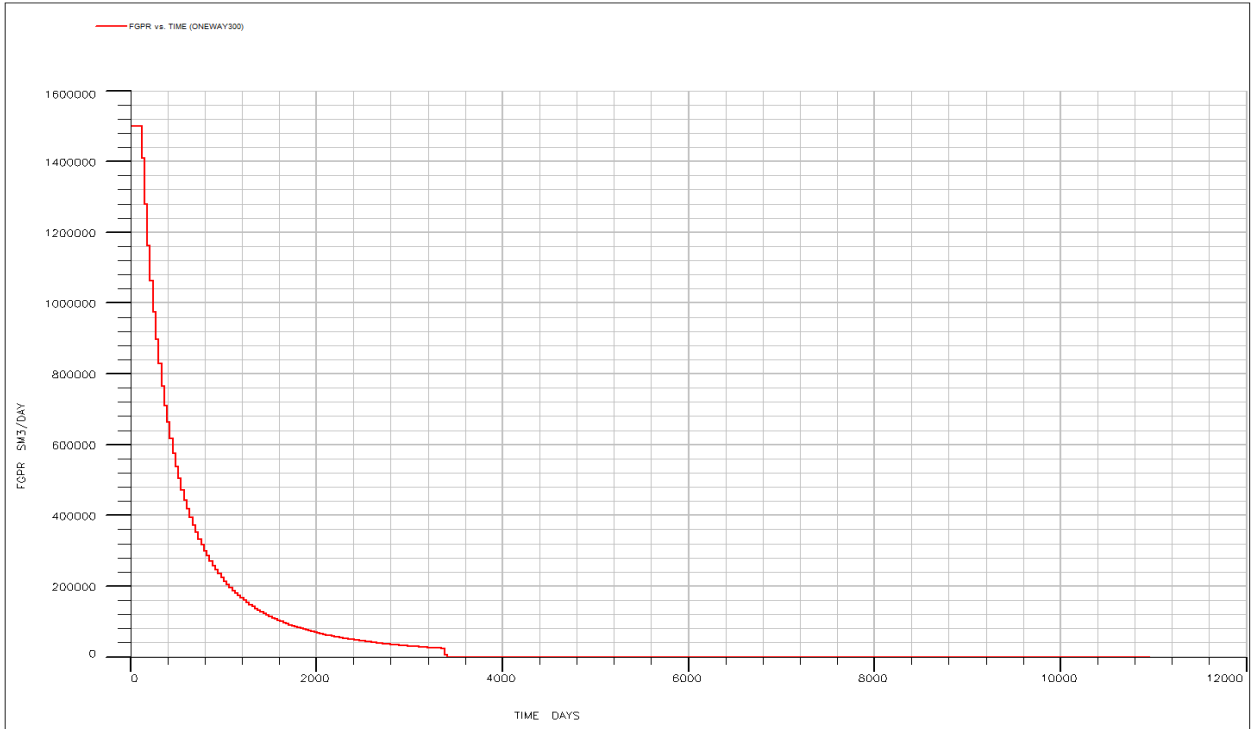


Figure 36 Cumulative Gas Production with respect to Time One Way Coupling

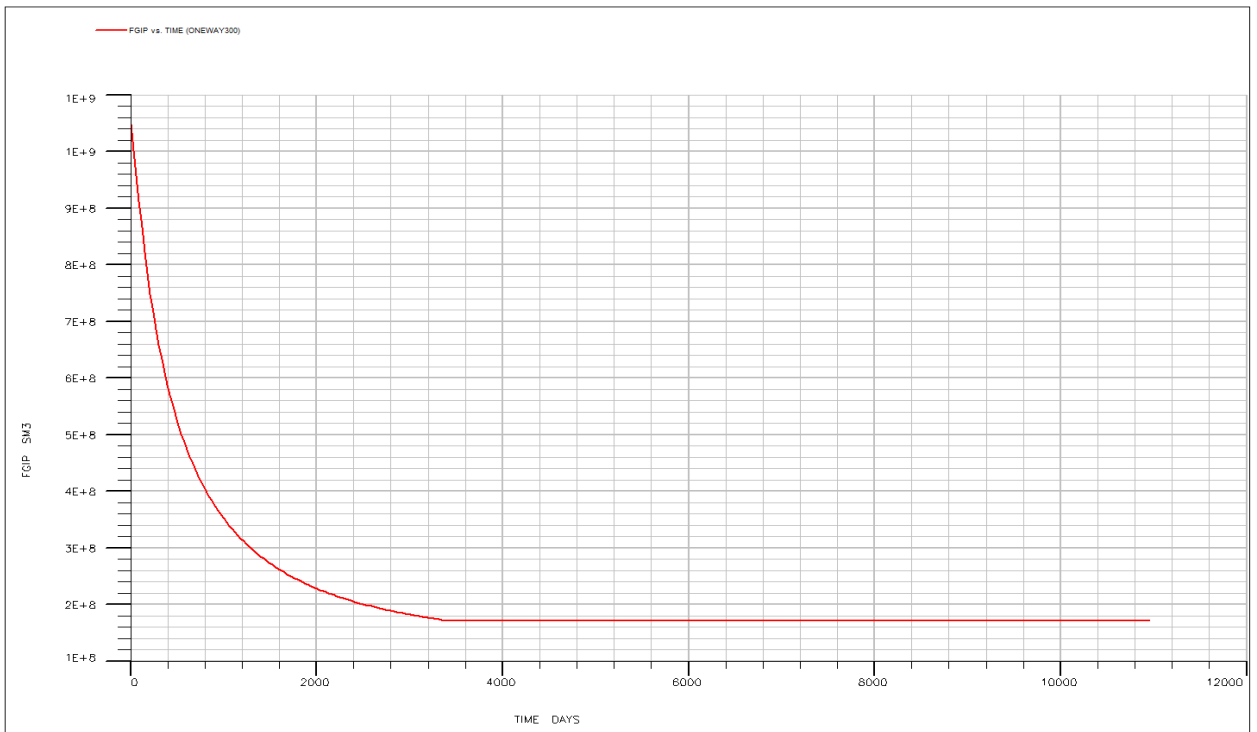


Figure 37 Gas in Place with respect to time One Way Coupling

Figure 36 shows the cumulative production rate of all 4 wells in the system from the beginning of production on the 1st of January 2016 which starts at 1500000 m_{sc}/day then a few months later starts to gradually decrease until production is shut on the 1st of May 2025. The production period is 9 years and 4 months, the same period as the one used for Case 1. Figure 37 shows the field gas in place starting from the beginning of production and the remaining gas in place at the end of production. The system reaches a recovery factor of about 88%.

B- One Way Coupling data

i-Shallow Depth Reservoir Geomechanics Simulation Data

Like Case 1, rock displacement and subsidence is displayed in order to determine its intensity. In this section, the results are going to be compared with the results of case 1 to see how different geomechanical compaction can be when decreasing the depth of the reservoir.

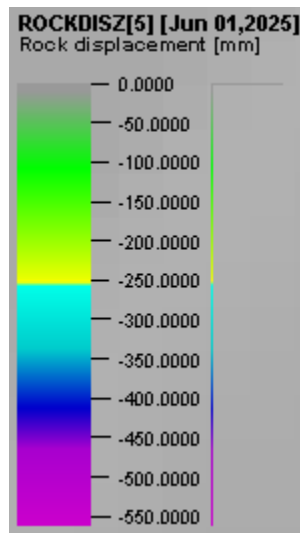


Figure 38 Legend showing intensity of Rock Displacement in millimeters for figures 37 40 and 42

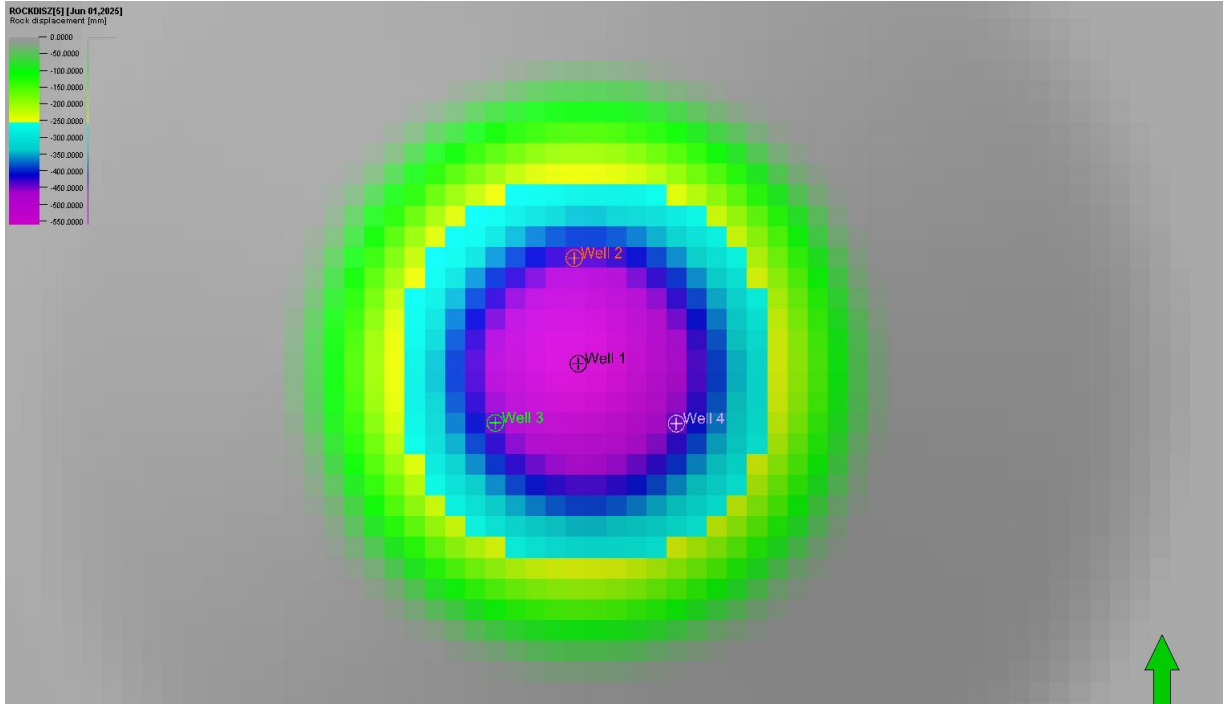


Figure 39 Rock Vertical Displacement in the Reservoir

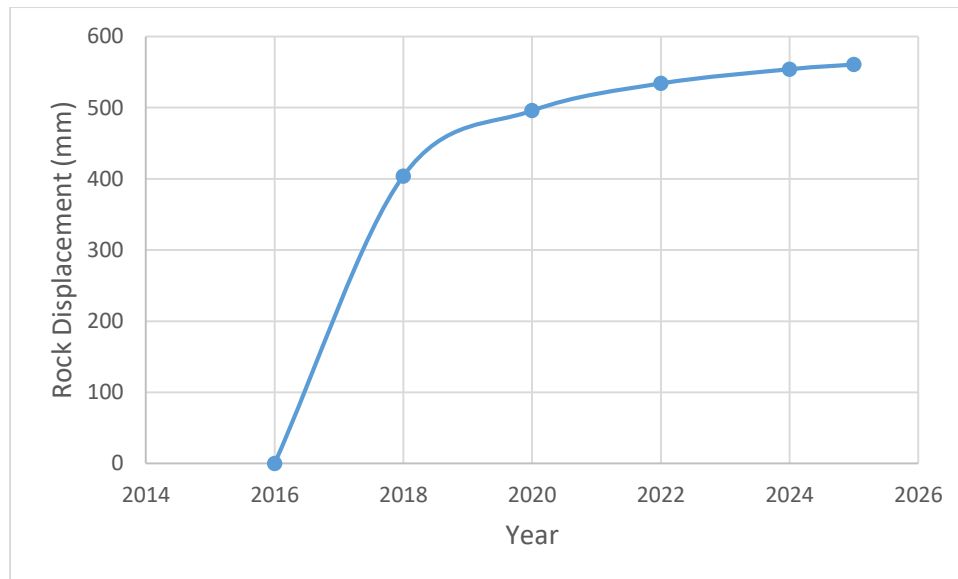


Figure 40 Reservoir Rock Vertical Displacement with respect to Time

In figure 39, rock displacement due to compaction in the reservoir is presented. Maximum rock displacement of 560 mm is reached. This is not too far away from the displacement reached at the reservoir of case 1. The reason behind the indifference is that the difference in depth is compensated by difference in young modulus primarily. In case 1, the reservoir rock has a young modulus of 1 bar, while for the the reservoir of case 2, the rock has a young modulus of 0.2 making it highly compressible.

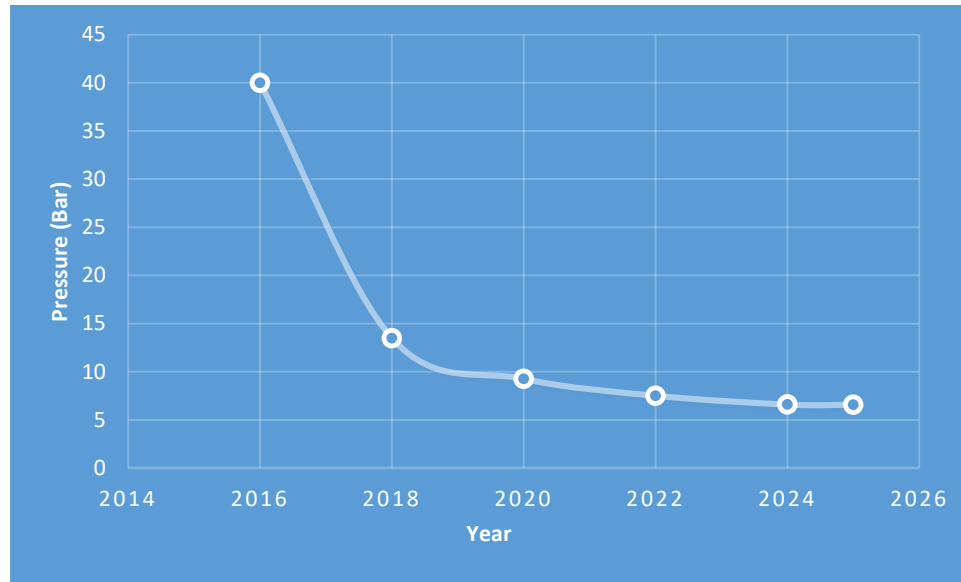


Figure 41 Pressure Decline Curve

As we can see in figure 41, the pressure of the reservoir is initially 40 bars and it starts to decline as production proceeds and reaches a value of 6.58 bars at the end of production in May of 2025. The pressure value reached at the end of production is 17% of the initial pressure, while the pressure reached at the end of the one way coupling approach of case 1 is about 7% of the initial pressure. Also, the pressure decline in case one is more of a linear behavior while in this case the behavior seems to be abrupt in the first two years then slowly stabilizes till the end of production in year 2025, forming a parabolic shape.

ii-Shallow Depth Surface Geomechanics Simulation Data

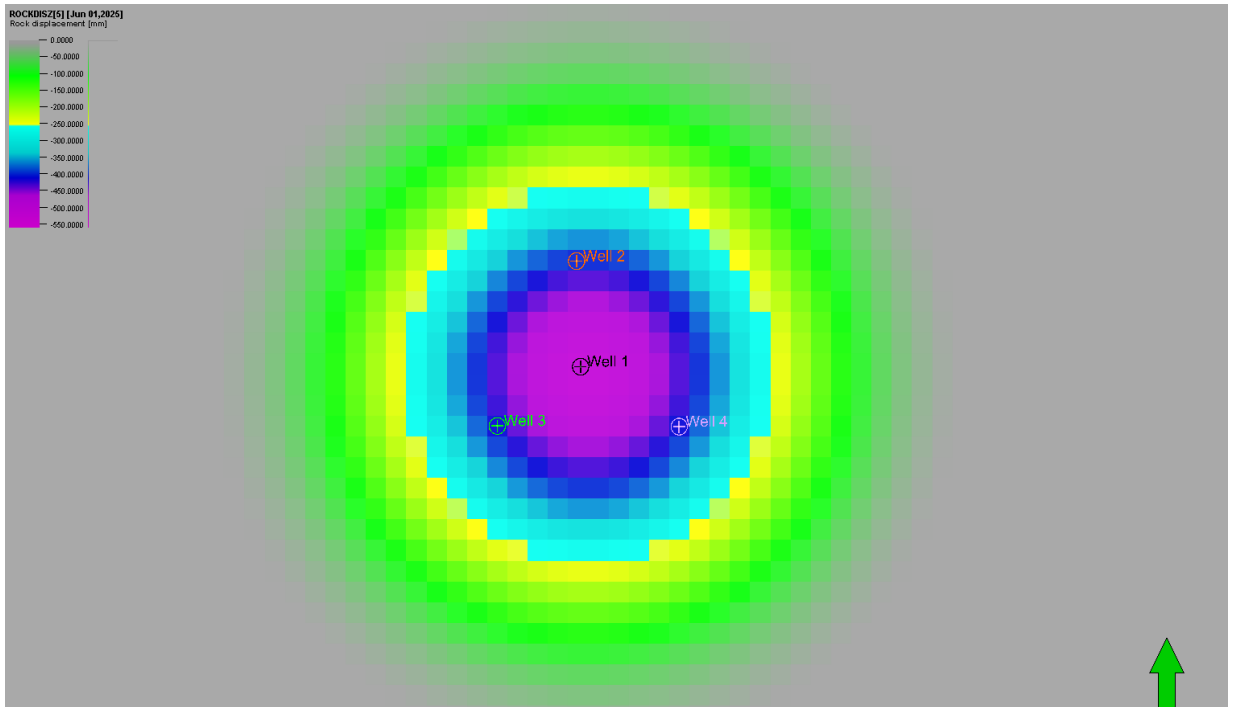


Figure 42 Surface Subsidence

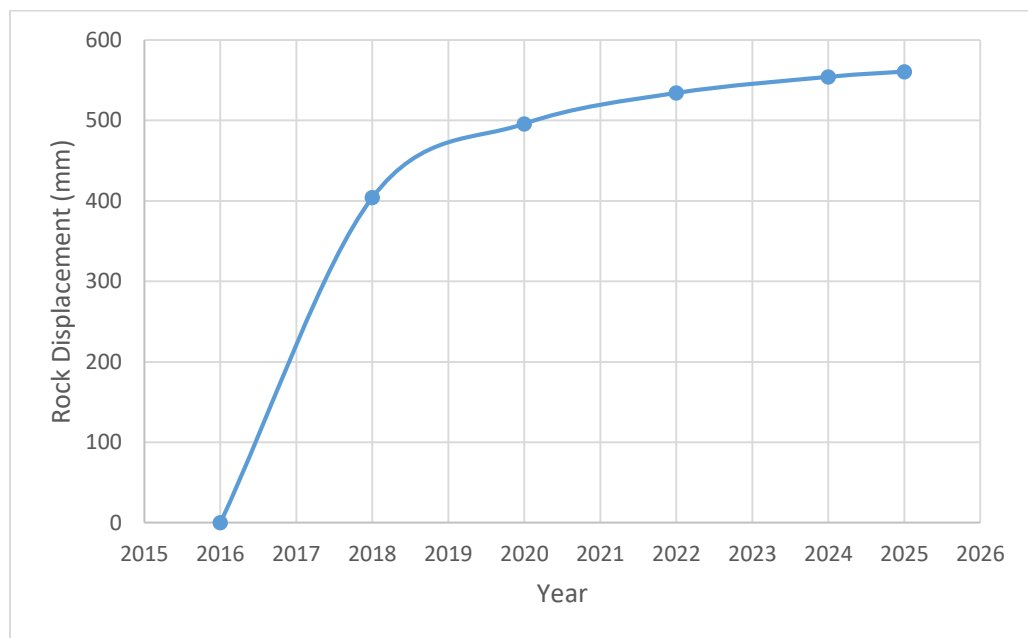


Figure 43 Surface Vertical Rock Displacement with respect to Time

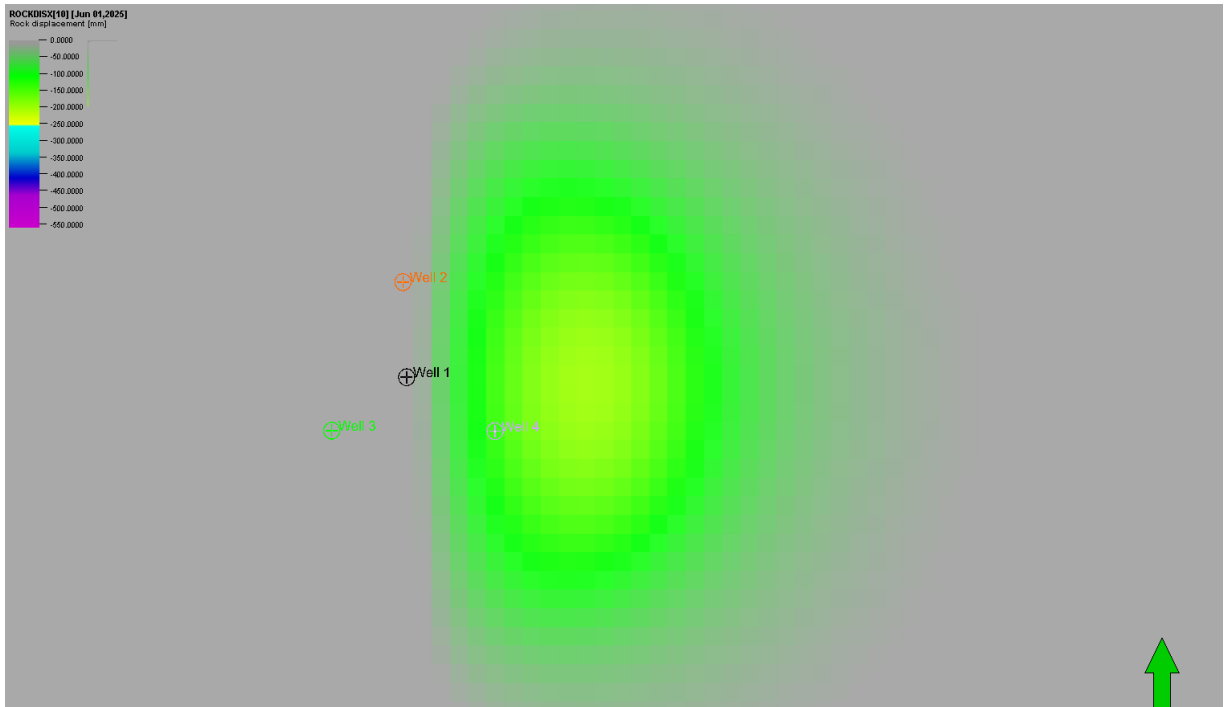


Figure 44 Rock Displacement in the Horizontal Direction

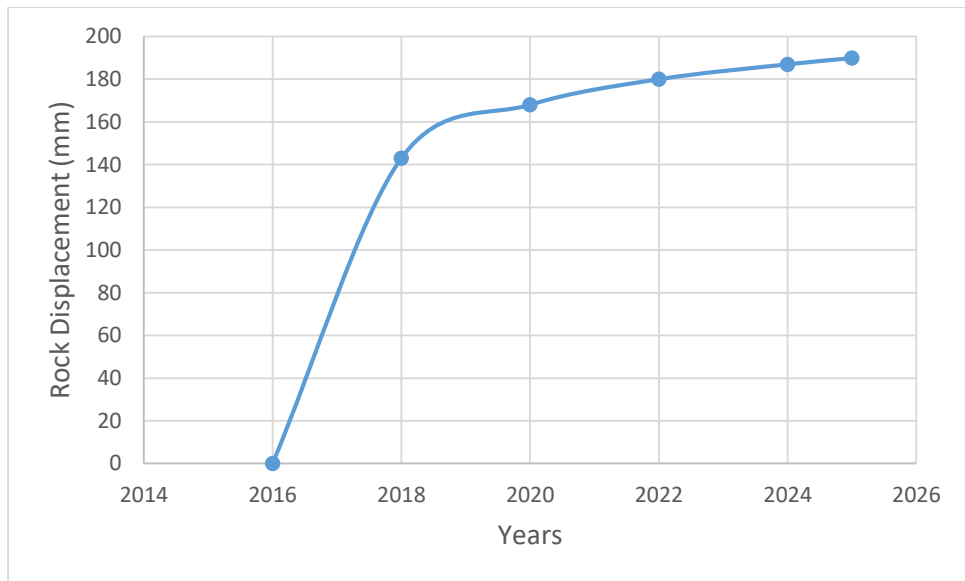


Figure 45 Rock Horizontal Displacement with respect to Time

Figure 42 to 45 show the subsidence at the surface caused by the reservoir rock displacement. The rock compaction on the reservoir scale might be very similar to the case of the medium depth reservoir, but that does not mean that the surface subsidence is the same. In fact, due to the reservoir being very shallow, the rock displacement in the reservoir is about 90% reflected at the surface reaching a maximum of 508 mm of rock displacement. This value is significantly higher than the one reached by the reservoir at medium depth which only reflects about 45% of reservoir compaction.

Table 2 Shallow Depth Reservoir Rock Displacement vs Surface Subsidence vs Subsidence Impact Radius

Time Step	Reservoir Maximum Rock Displacement (mm)	Surface Subsidence (mm)	Subsidence Radius (m)
2016	0	0	0
2018	404	362	1438
2020	496	447	1537
2022	534	483	1637
2024	554	501	1637
2025	561	508	1638

As stated previously in Case 1, the amount of surface subsidence reflected from reservoir rock compaction depends on the reservoir’s lateral extension, depth and the characteristics of the overlying rock. Since this reservoir is very shallow and the overlying rock have a very low young modulus of < 0.2 , the reservoir rock displacement is highly reflected at the surface with about 91% of reservoir rock displacement being translated into surface subsidence as seen in table 2.

Table 2 also shows the radius of surface subsidence impact which is about 1638 meters by the end of production. Since the reservoir is shallow and close to the surface, the subsidence radius tend to not go far away from the lateral extent of the reservoir.

C- Two Way Coupling

Similar to Case 1, two way coupling results are displayed using different equations for reservoir fluid flow calculations. For each method, three reservoir production data are displayed; remaining gas in place, well cumulative production rate and pressure decline curve. In addition, permeability decline curves are also presented to demonstrate how each method leaves its mark on permeability decline.

Kozeny-Carman

Results using this method are displayed below;

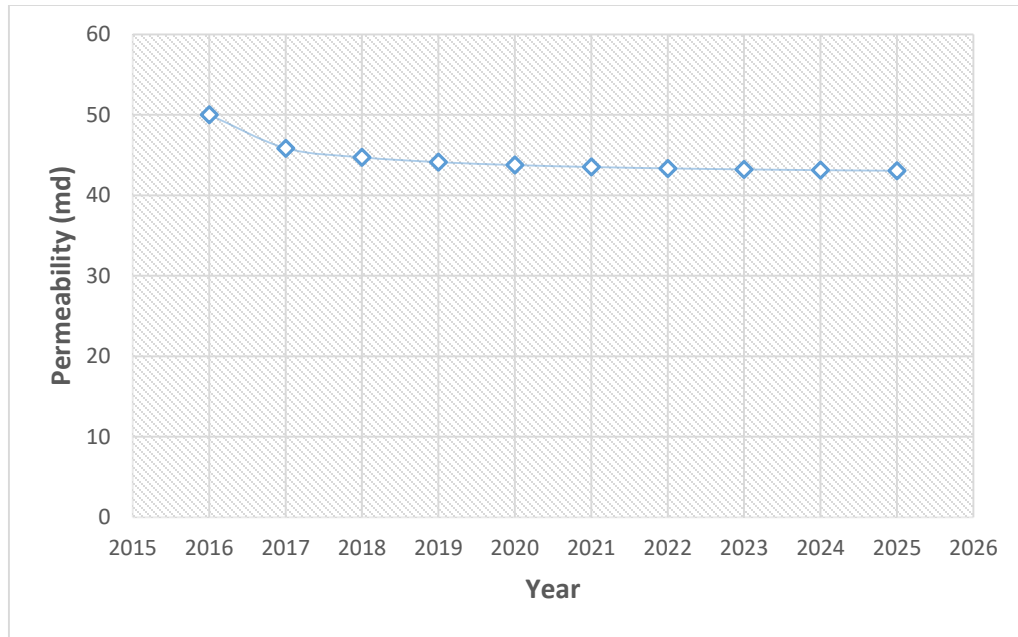


Figure 46 Permeability Decline Kozeny-Carman

Visage, as shown in case 1, uses strain to update porosity thus calculating permeability based on the equation assigned. In this case the Kozeny-Carman equation was used to determine the change in permeability and thus the change in production data. As it can be seen in figure 46, the permeability starts at 50 mD in the beginning of production and ends at about 43 mD.

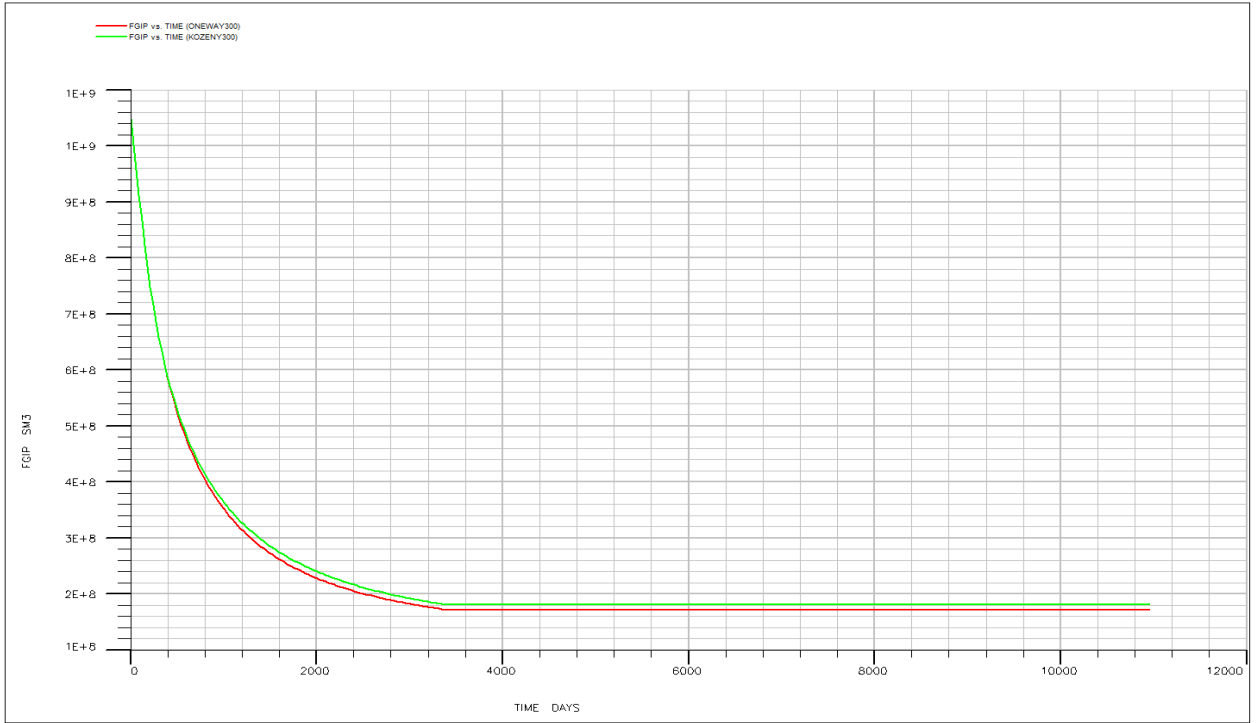


Figure 47 Gas in Place with respect to time One Way Coupling (RED) Kozeny Carman (GREEN)

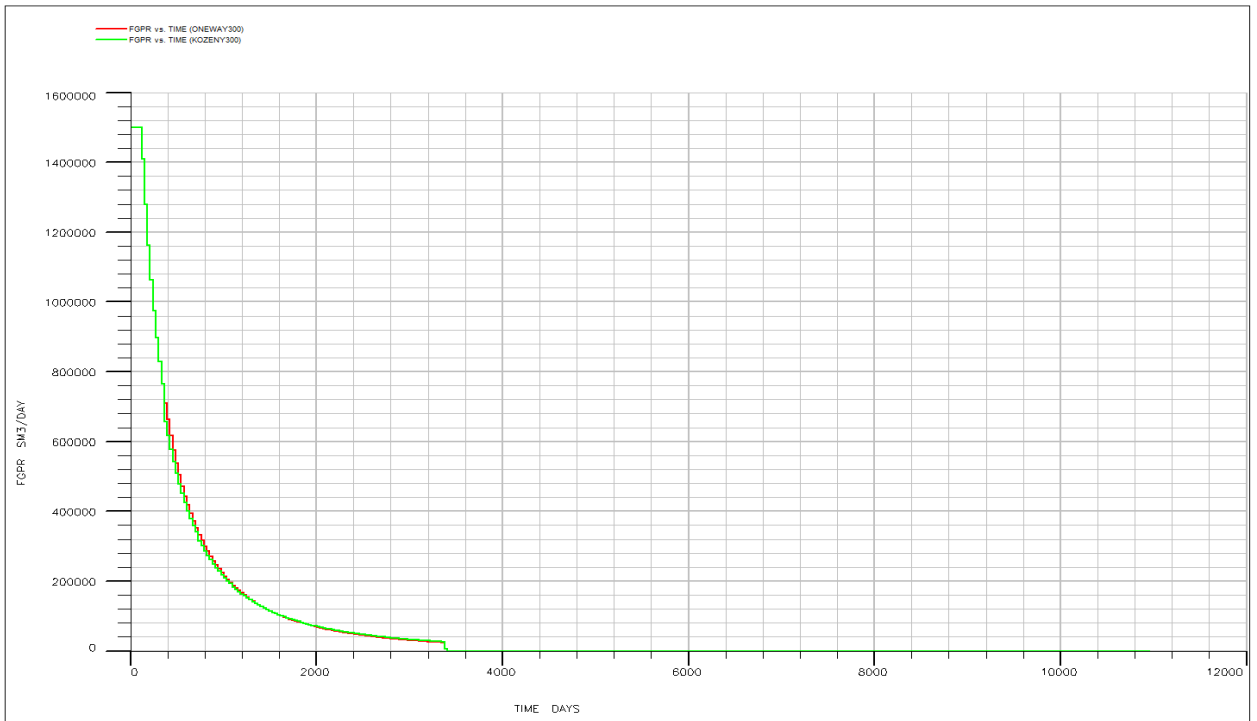


Figure 48 Cumulative Gas Production with respect to Time One Way Coupling (RED) Kozeny Carman (GREEN)

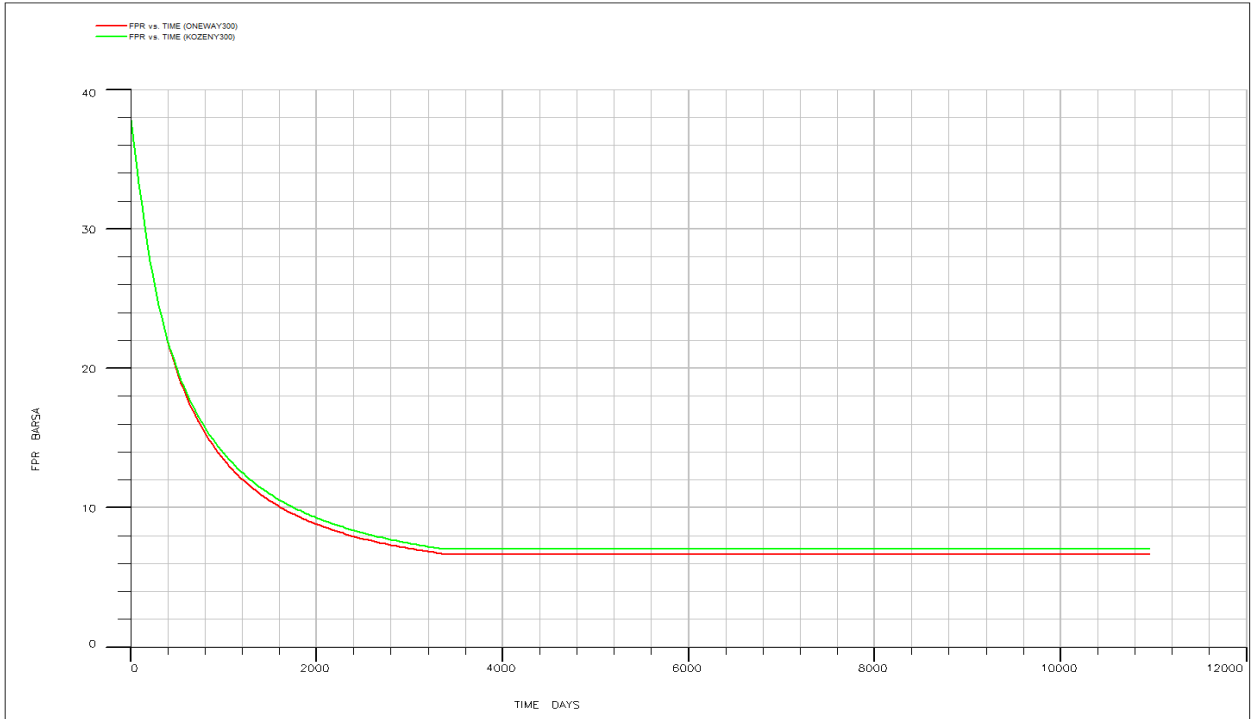


Figure 49 Pressure Decline Curve One Way Coupling (RED) Kozeney Carman (GREEN)

Figures 47 and 48 show clearly that the 10 mD decrease in permeability barely affects production data. As it can be seen, the curves are only slightly off superposition which means that there is no significant change neither in recovery factor nor in well production rate nor reservoir pressure. In addition, figure 49 shows that there is no real difference in pressure at the end of production between the two coupling cases.

Polynomial Law

Results using this method is displayed below;

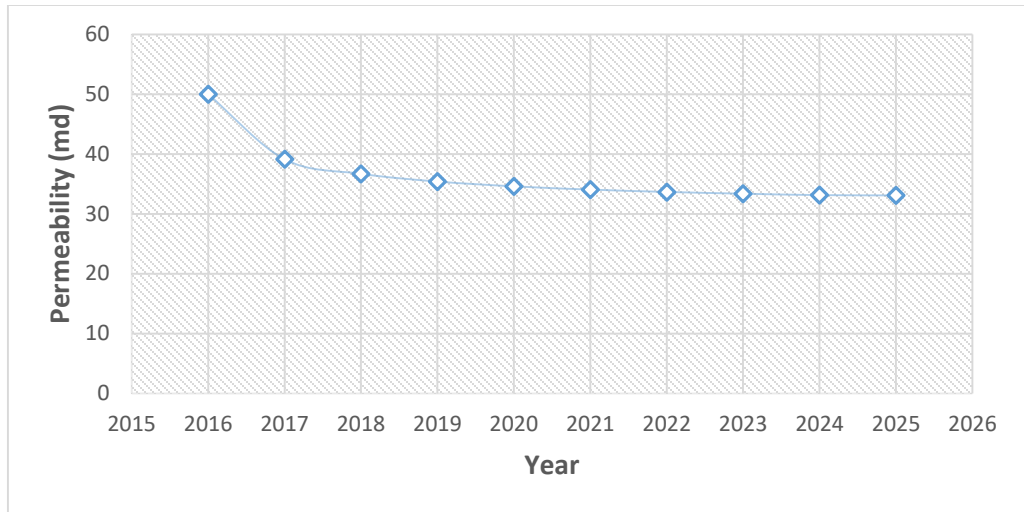


Figure 50 Permeability Decline Polynomial Law

Figure 50 shows the permeability decline in the reservoir while simulating the two way coupling approach using the polynomial law as a permeability update equation. As it can be seen, permeability decline is significantly more aggressive than the Kozeny-Carman case and reaches a value of 33md at the end of production. This permeability decline is used in order to determine its effect on production data.

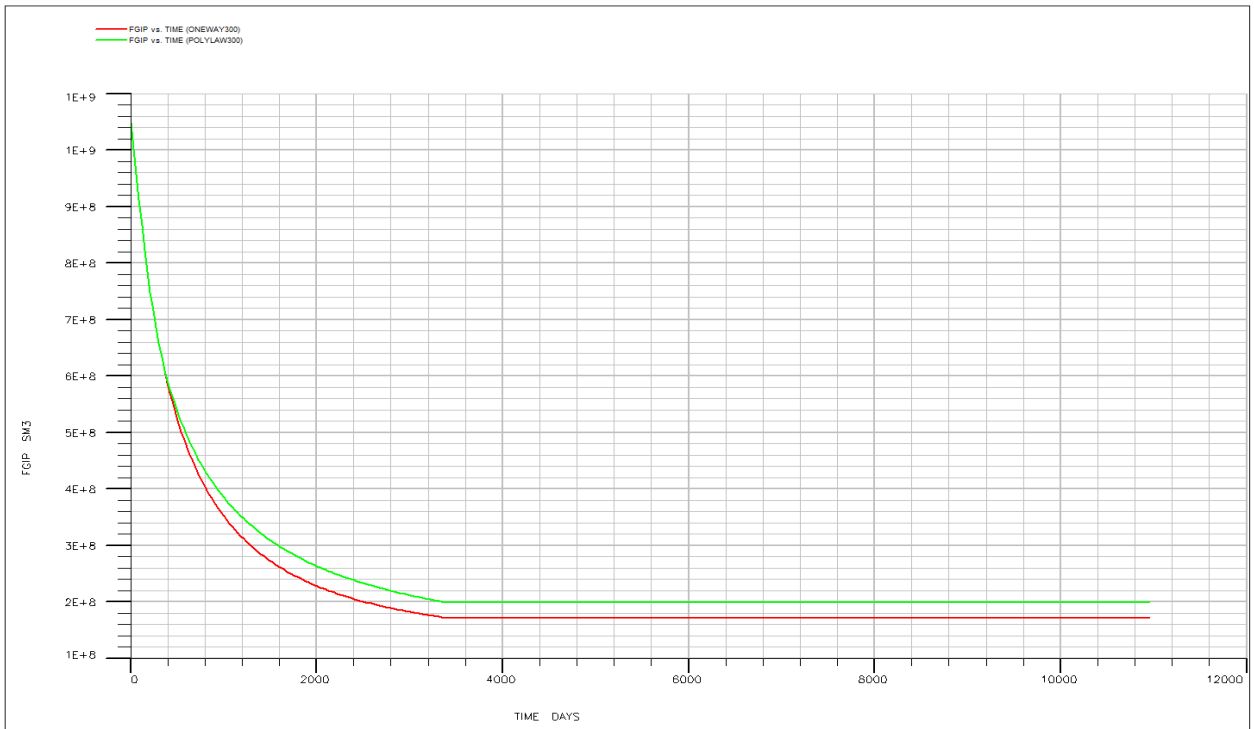
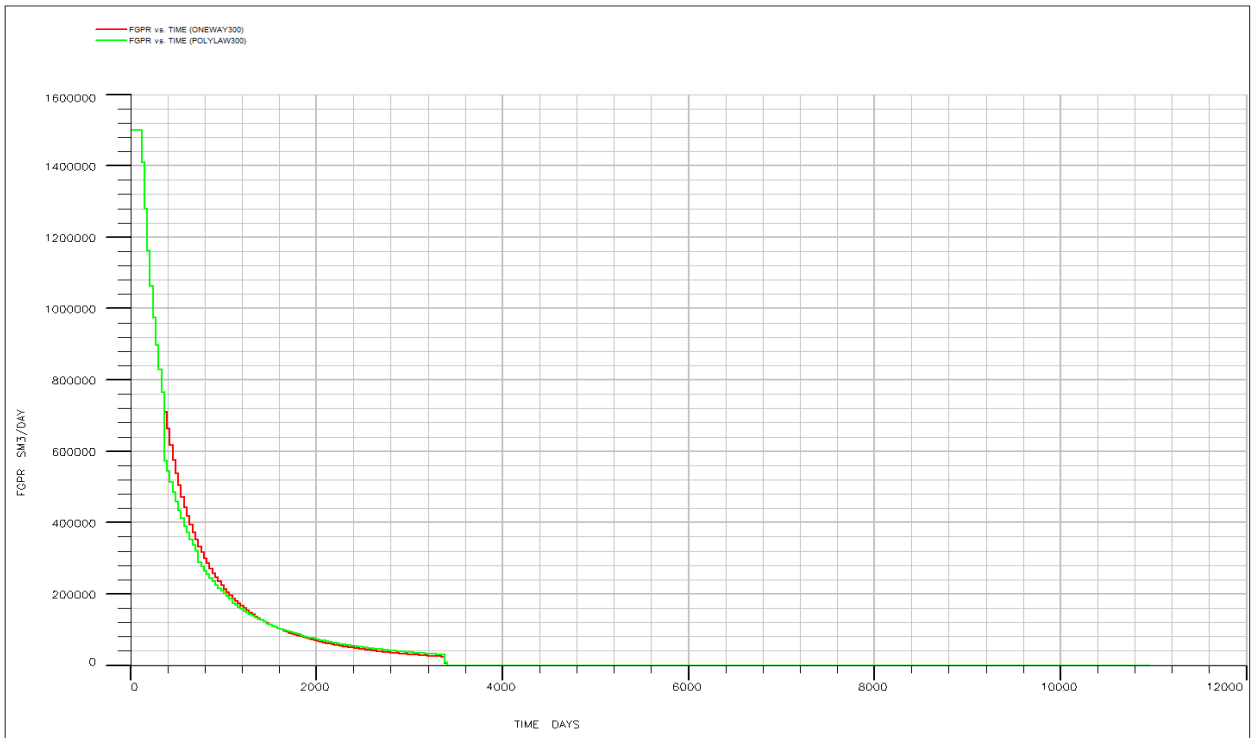


Figure 51 Gas in Place with respect to time One Way Coupling (RED) Polynomial Law (GREEN)



*Figure 52 Cumulative Gas Production with respect to Time One Way Coupling (RED)
Polynomial Law (GREEN)*

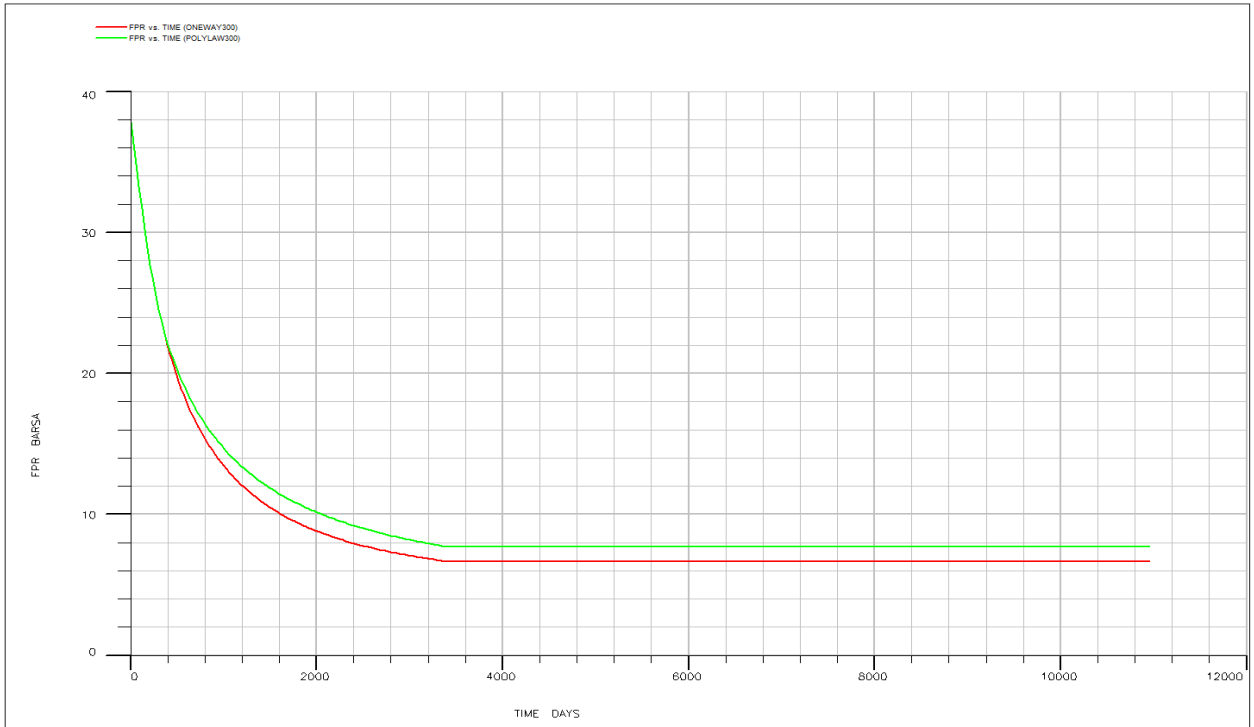


Figure 53 Pressure Decline Curve One Way Coupling (RED) Polynomial Law (GREEN)

Production data has slightly been affected using the polynomial law in comparison with the one way coupling simulation. As it can be seen in figure 52, cumulative well production has been hindered, even if not at a very aggressive level. Remaining gas in place increase to $2 * E^8 \text{ sm}^3$, as seen in figure 47, so the recovery factor decreased to about 85.7 % which is not too significant. The pressure of the reservoir at the end of production was also slightly increased by about 2 bars in comparison to the one way coupling approach which is also a very mild increase, as seen in figure 49. Even though this more aggressive permeability decline did affect the production data, but it is not enough to produce significant changes.

Intact Porosity Table

Results using this method are displayed below;

In this method, lab data were used in order to represent the behavior of the permeability decline with changes in porosity. The lab data used is the same as the one used in Case 1, which is represented in figure 29.

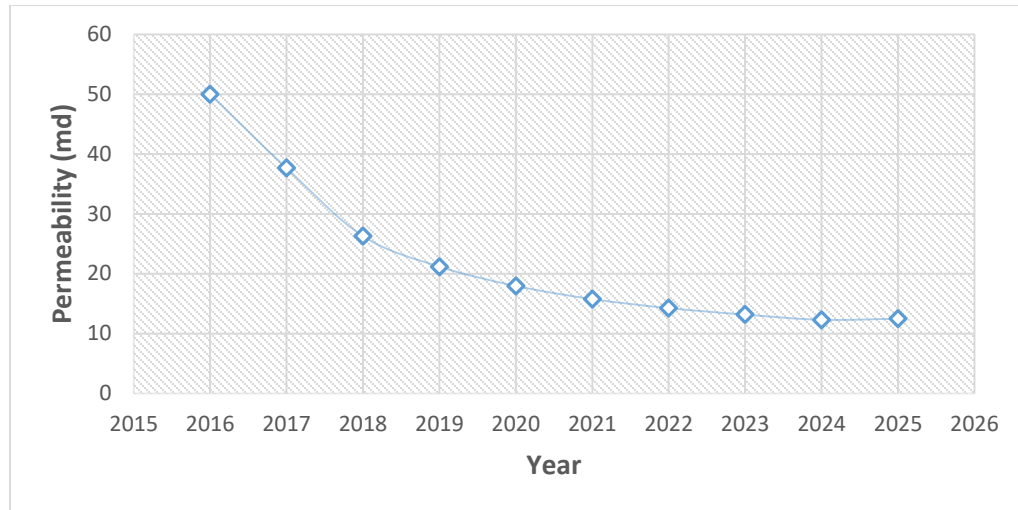


Figure 54 Permeability Decline Intact Porosity Table

Figure 50 represents the permeability decline curve of our reservoir during production using the function created out of the inserted lab data as discussed above. The permeability decreased in an abrupt way from 50 mD to about 12.5 mD, which is just 2.5 mD away from a one order of magnitude decline. This intense decrease is due to the extreme lab data inserted in order to demonstrate what could happen to the reservoir in case of abrupt permeability decline.

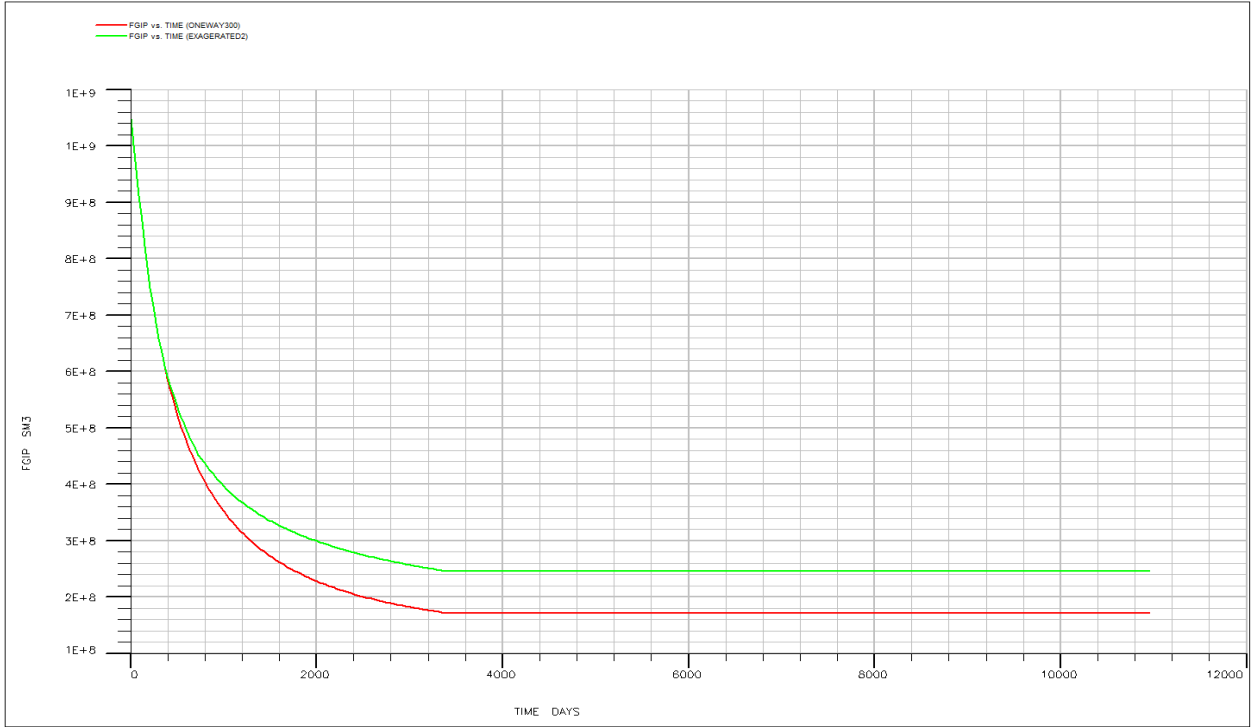


Figure 55 Remaining Gas in Place with respect to time One Way Coupling (RED) Intact Porosity Table (Green)

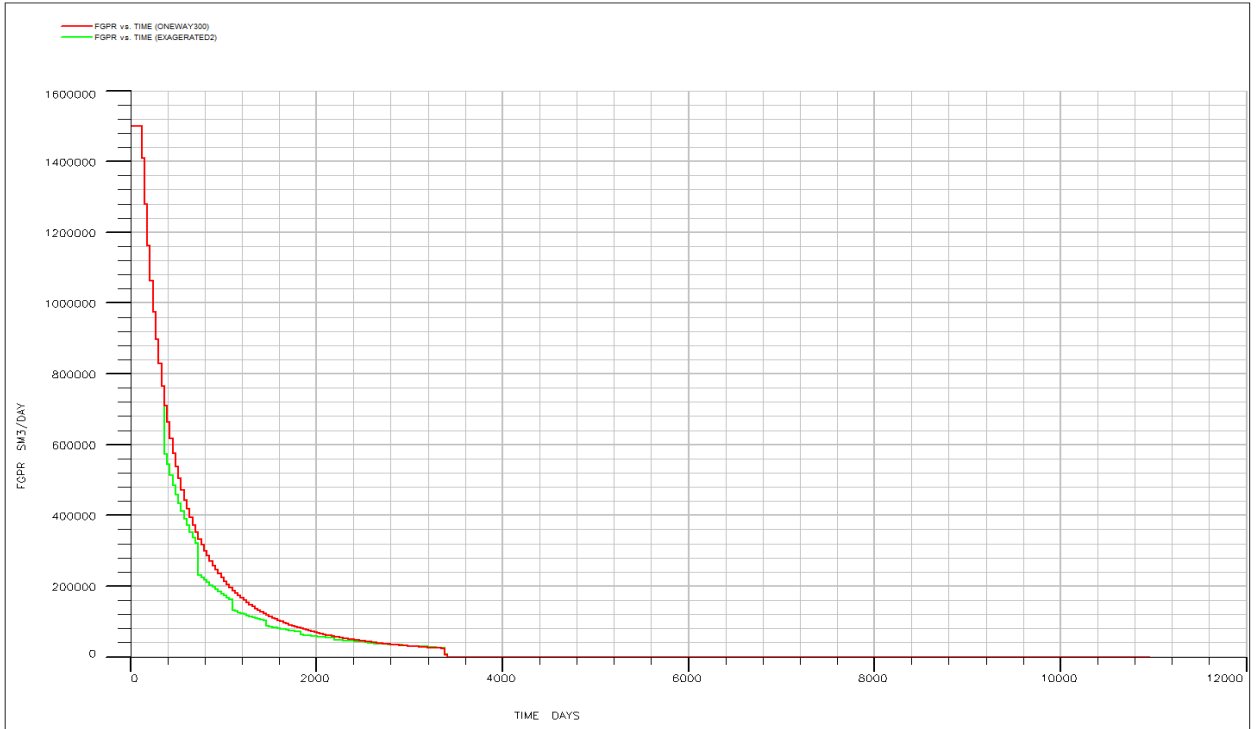


Figure 56 Cumulative Gas Production with respect to Time One Way Coupling (RED)
Intact Porosity Table (Green)

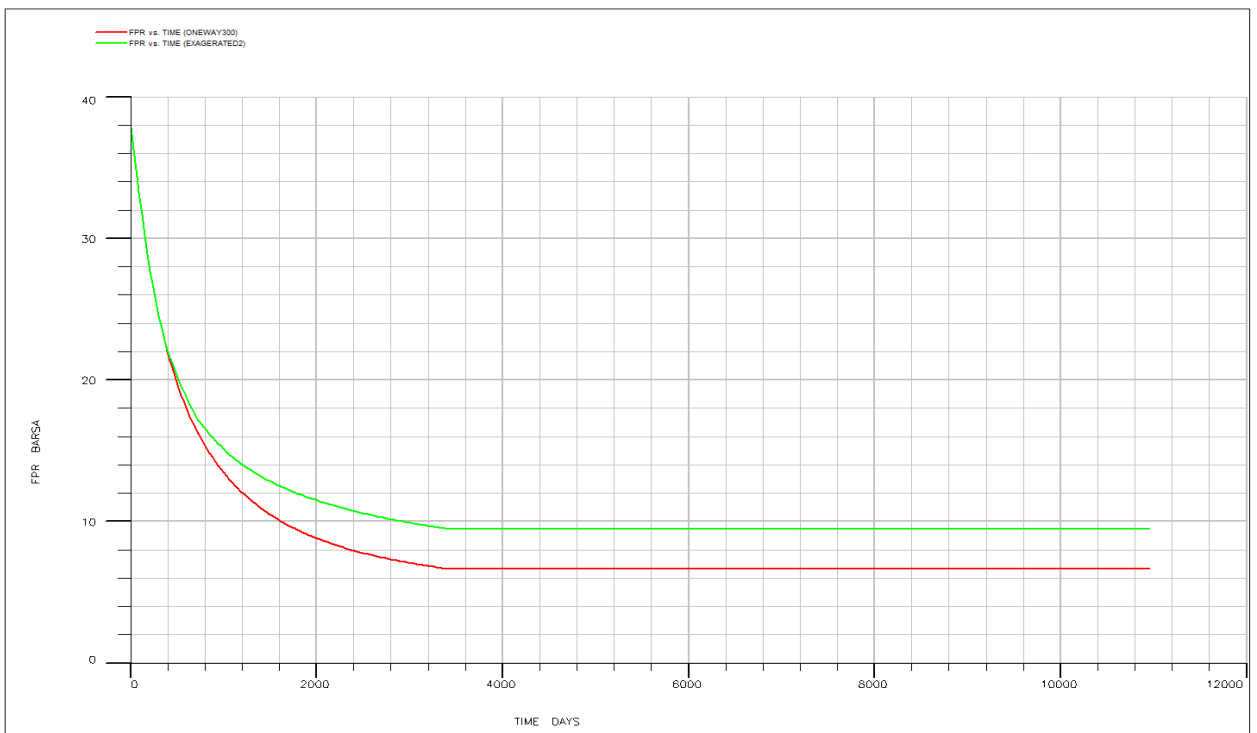


Figure 57 Pressure Decline Curve One Way Coupling (RED) Intact Porosity Table (Green)

As it can be seen in figure 56, cumulative production was significantly hindered by the abrupt decrease in permeability. This decrease in well cumulative production led to the increase of remaining gas in place, as seen in figure 57, at the end of production to about $1.7 * 10^8 sm^3$, which as a result caused a decrease in recovery factor to about 82%. This increase in remaining gas in place resulted in a 3 bar increase in reservoir pressure in comparison to the one way coupling approach, leaving it at 9.5 bar as it can be seen in figure 55.

Chapter 4: Discussion and Comparison

The data simulated in chapter 3 is very important for understanding the level of importance of two way coupling. After choosing the production data as our basis for the study in case 1 and 2, the simulations were run and the results were obtained. The one way coupling results obtained in part B of the case study, not only provided us crucial surface subsidence information but also allowed us to use the production data and the results as a basis for comparison with other coupling techniques used in the two way coupling approach.

A- Subsidence

When one way coupling results were calculated for both cases, it was realized that both reservoirs have about the same amount of reservoir compaction. This is because in case 2, the difference in depth was compensated by decrease in young modulus to about 0.2 in comparison to a value of 1 in case 1. This value of young modulus allows for a more intense compaction results.

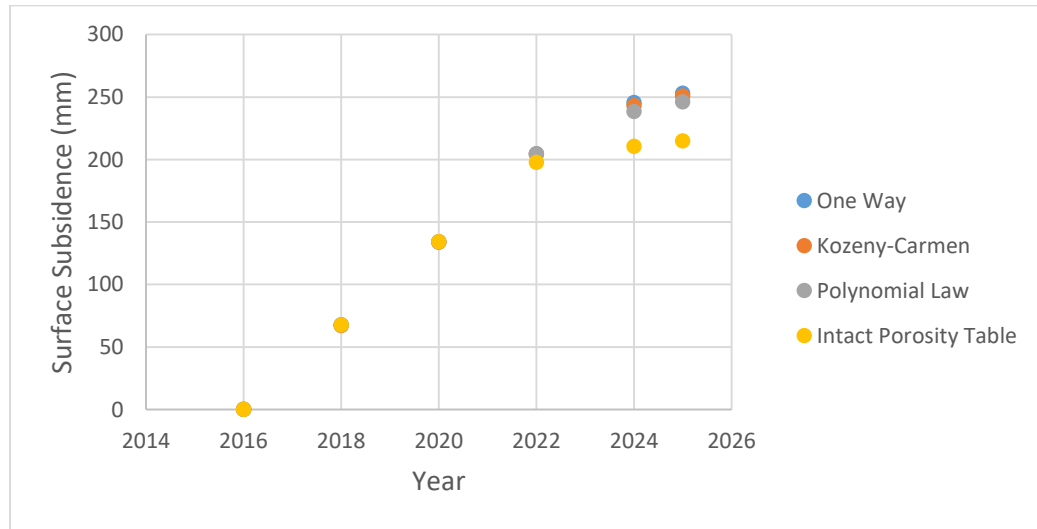


Figure 58 Surface Subsidence For all Coupling Methods of Case 1

Figure 58 displays all the subsidence trends followed based on all different coupling methods for Case 1, the lab data represented by the intact porosity table is the farthest from the one way coupling data. The Kozeny-Carman simulation shows to have the closest surface subsidence value to the one way coupling approach with a devaluation of about only 0.8%. The polynomial law approach also has a small devaluation value of about 2.4%. On the other hand, as it can be seen in part C, the intact porosity table method is the method with the most discrepancy with the one way coupling method, which showed a considerable amount of 15% devaluation in surface subsidence comparing to one way coupling. This is due to the abrupt decrease in permeability due to compaction, thus hindering field production capabilities.

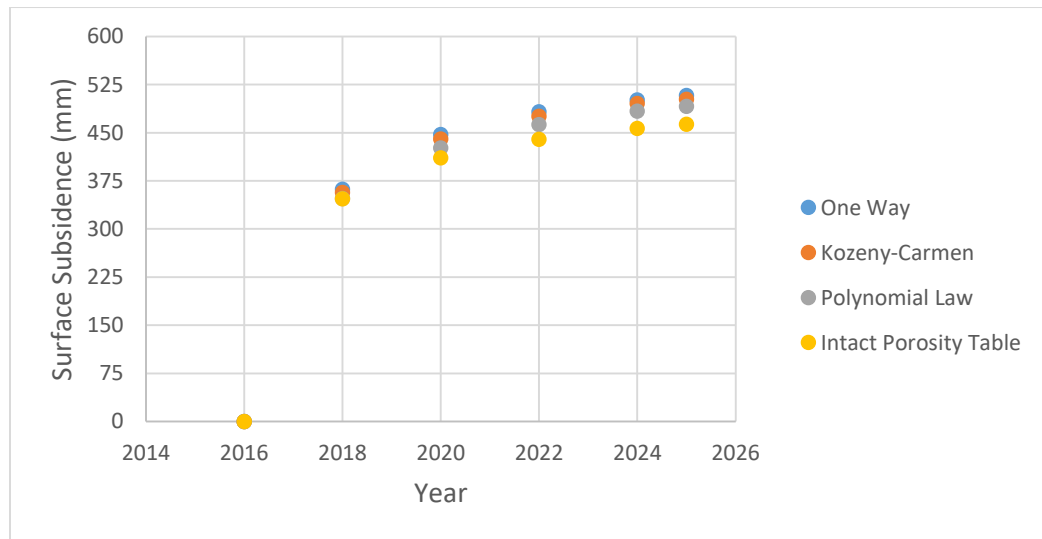


Figure 59 Surface Subsidence Results For Each Coupling Method of Case 2

Figure 59 represents the surface subsidence value found after simulating based on different coupling approaches of Case 2. The lab data represented by the intact porosity table is the farthest from the one way coupling data, similar to what was seen in the case 1 simulation. This is due to the abrupt decrease in permeability, thus hindering field production capabilities. The Kozeny-Carman simulation seems to have the smallest surface subsidence devaluation when compared to surface subsidence value of the one way coupling approach with a devaluation of about only 1.23%. The polynomial law approach also has a small devaluation value of about 3.3%. Looking at the intact porosity data shows to have a noticeable discrepancy with the one way coupling data which has a devaluation value of about 8.7%. In addition, comparing case 1 and case 2 we can see that the subsidence results for all the coupling methods in case 2 start to differ after 2 years of production, unlike in case 1 where the difference starts to show only after 6 years of production.

As it can be seen in figures 58 and 59, the two way coupling approaches tend to have less surface subsidence than the one way coupling approach. Consequently, less production means more fluid in the reservoir which also means less compaction in the

reservoir and therefore on the surface. Having stated the data, one can come to the realization that two way coupling could make subsidence results a bit more accurate, but the difference is not very significant, even in the exaggerated cases. As a conclusion, we can safely say that the one way coupling approach can always be used for accurate subsidence interpretation.

To better understand the differences between having the same reservoir at different depths, data showing Surface Subsidence difference and Surface Subsidence impact radius are displayed below in figure 60.

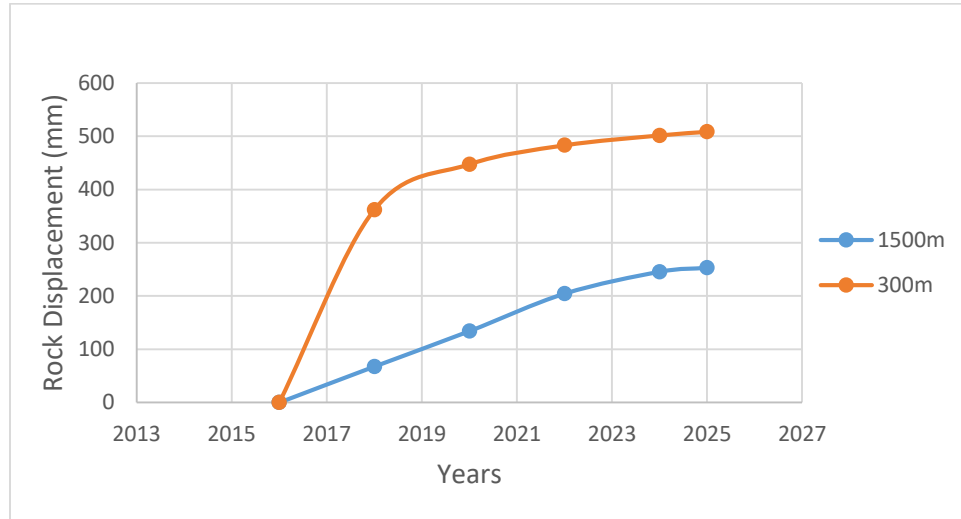


Figure 60 Surface Subsidence 300m vs 1500m

Since both reservoirs experience very close values of rock compaction, it is feasible to compare surface subsidence between the two reservoirs. As expected, surface rock displacement is much higher in case 2 rather in case 1 due to the reservoir's much shallower depth. The closer the reservoir is to the surface the more reservoir rock compaction reflects on the surface subsidence.

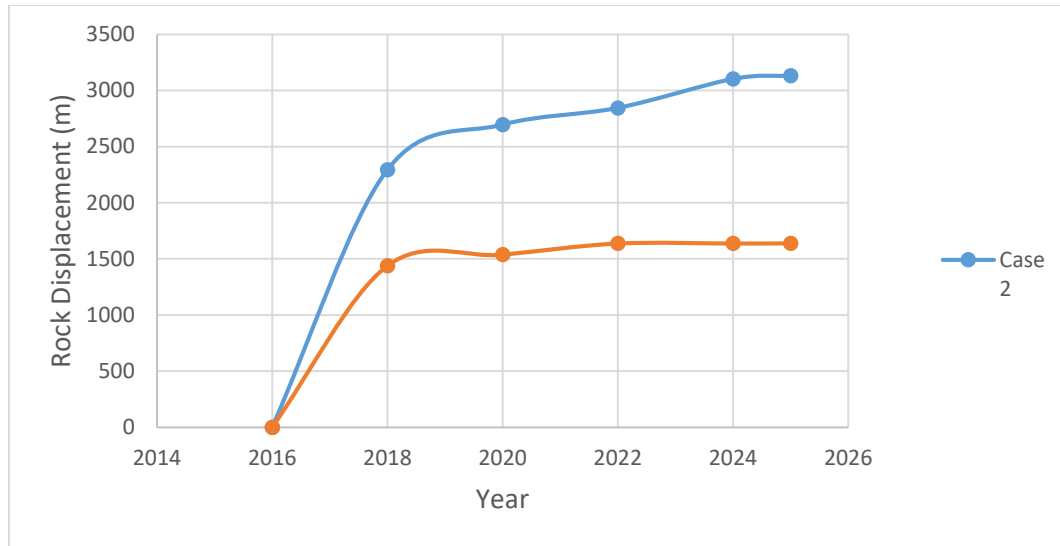


Figure 61 Case 1 Surface Subsidence Radius vs Case 2 Surface Subsidence Radius

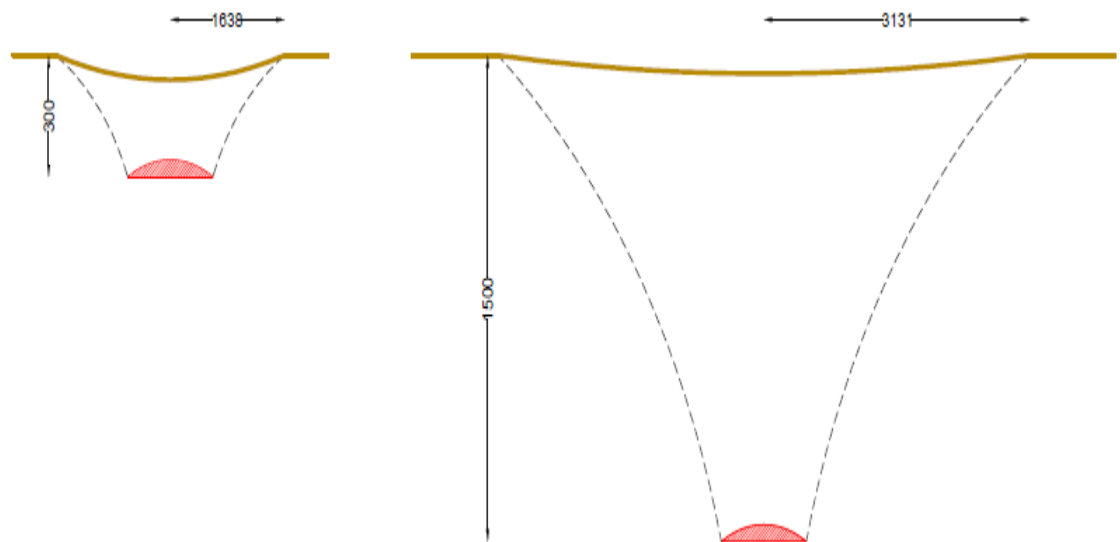


Figure 62 Subsidence Representation

Figure 61 shows the Difference in subsidence impact radius at the surface for both medium depth and shallow depth reservoirs. Even though the impact intensity at the surface is much greater in the shallow reservoir than in the medium depth reservoir, the radius of impact is 1638 meters for case 2, about half the subsidence radius of case 1 which is about 3131 meters. Figure 62 is a representation of the radius of influence each subsidence case causes at the surface.

B- Production Data

As previously discussed in previous chapters, after simulating the two way coupling methods, change in production data was expected. In both cases 1 and 2, we noticed change in production data when implementing different permeability decline equations and functions. Permeability decline in the reservoir was quite noticeable as it can be seen in chapter 3, but also quite different when going from one method to another. Nonetheless, even though permeability decline was somehow significant in every method, in some method it wasn't enough to induce a strong impact on production data. We noticed that when implementing the permeability decline equations, Kozeny-Carman and Polynomial law, only a small change in production data was observed. On the other hand, when using the intact porosity table function derived from lab data analysis, the change in production data was quite appreciable.

Table 3 Permeability Percent Change at the end of production

	Kozeny-Carman	Polynomial Law	Intact Porosity Table
Case 1	13%	33.8%	75%
Case2	18%	42%	91%

Table 3 shows the percent decrease of permeability at the end of production for every method used for every case with respect to original permeability of 50 mD at the beginning of production. As previously discussed, the permeability decrease is quite noticeable in all the different cases but at different degrees. The permeability decline of the Kozeny-Carman method and Polynomial law method for both cases seem to be close to each other, although a bit higher for case 1 since the system experiences a slightly higher volumetric strain which would consequently cause a higher decrease in permeability. On the other hand, for the intact porosity method the permeability decline percentage for both cases are high due to the inserted permeability vs porosity table inserted originally. In addition, we realize that the correlation that has the least impact on permeability and thus production data is the Kozeny-Carman correlation. The Polynomial law has stronger permeability decline results because a porosity exponent of 10 was chosen in order to test the reservoir to the maximum.

Table 4 Percent Decrease in Recovery Factor

	Kozeny-Carman	Polynomial Law	Intact Porosity Table
Case 1	<0.5%	2.1%	12.5%
Case2	<0.5%	2.6%	6.8%

Table 4 shows the change in recovery factor for both cases 1 and 2 with respect to their original recovery factor of 92.5% and 88% respectively. As we can see, recovery factor for both cases using Kozeny-Carman and the Polynomial law was quite similar and relatively low. Even though, for the polynomial law case, a 2.1% and 2.6% of the recovery factor means about $8.16 * 10^7 sm^3$ for case 1 and $3.2 * 10^7 sm^3$ of gas. On the other hand, the intact porosity table method has much more appreciable results. Even though one must keep in mind that comparing the two cases on the basis of lab data can't be done since the same data used for case 1 was used for case 2 which is not the case in real life and was only done for the sake of experimenting, we realize that this data has big results that can cause big losses in gas production. For case 1, the 12.5% decrease in recovery factor means a loss of $4.85 * 10^8 sm^3$ of gas. For case 2, a 6.8% decrease in recovery factor is anticipated and this means a loss of $8.377 E^7 sm^3$.

Chapter 5: Conclusion

Reservoir production data and reservoir simulation were historically the main issues exploited by petroleum engineers. Then the geomechanical issue immersed when in particular cases, subsidence problems started to immerge hence one way coupling simulations were introduced in order to simulate surface subsidence results. Then came the question, can reservoir rock compaction due to production cause the fluid flow capabilities of the reservoir to be altered? The focus of the thesis is to evaluate the effect of coupling techniques between fluid flow phenomena and geomechanical phenomena on both production results and subsidence estimation. Two coupling techniques were tested; one way coupling and two way coupling. In one way coupling, pressure and temperature changes are transferred from the reservoir simulator to the geomechanics model, but the geomechanics model does not transfer back any data to the reservoir simulator. This method is highly effective in situations where the reservoir fluid has a high compressibility, like in the case of gas reservoirs, while it could lead to faulty results where there is a strong relationship between reservoir fluid flow and porosity changes ^[14]. In two way coupling, reservoir simulators send pressure and temperature changes to the geomechanical model, which calculates the effects of rock deformation on porosity and permeability and sends them back to the reservoir simulator in order to simulate new pressure evolution trends.

The analyses were developed on two synthetic cases, the first case is a medium depth gas-reservoir at 1500m and the second case is a shallow gas-reservoir 300m. The petrophysical properties of both reservoirs are coherent with lithology (i.e clastic formation), while the initial conditions of both reservoirs are different. Geomechanical properties (such as unconfined compressive strength and the young modulus) are also coherent with the lithology and the in situ condition. The reason behind choosing the second case to be a shallow reservoir is to test the coupling simulations in an extreme case. For each case, the production conditions were chosen in a way to stress the system to the maximum in order to appreciate coupling effects. Consequently, one way coupling simulations were run for each case in order to monitor rock displacement at

the reservoir level and at the surface subsidence levels. In addition, two way coupling simulations using three different methods: Kozeny-Carman, Polynomial Law and Intact Porosity Table, were performed and different results were deduced for each case concerning both production and subsidence data.

In details, one way coupling simulations were done to obtain subsidence results and to use the production data as a basis for comparison with the two way coupling simulations. For case 1, the medium depth reservoir was subjected to production and at the end of production surface subsidence was about 45% of reservoir rock displacement. For case 2, the shallow depth reservoir experienced about the same reservoir rock displacement reached by case 1 since the depth difference between the two cases was compensated by the decrease in young modulus of the reservoir formation of case 1 and the difference in the imposed pressure drop. Surface subsidence in case 2 reflected almost 90% of reservoir rock displacement. The reason behind the difference in surface subsidence, knowing that both reservoirs have the same lateral extent, is that case 2 has a much shallower depth and thus the overlying rock is unconsolidated loose sand. In addition, surface subsidence radius was compared between the two cases and naturally the medium depth reservoir reflected a much higher subsidence radius than the subsidence radius experienced in the shallow depth reservoir.

When compared with the one way coupling method, the two way coupling simulations showed different and devaluated results in terms of cumulative production and recovery factors. In particular, even though the results for the Kozeny-Carmen and the Polynomial law equations showed a weak difference when compared with the one way coupling reservoir simulation data, there was a minor decrease in recovery factor because cumulative well production was slightly devaluated. In addition, reservoir pressure at the end of production was also at a slightly higher level than the one way coupling cases. Moreover, we also introduced permeability vs porosity lab triaxial compaction data into an intact porosity table which created a new function for the simulator to follow. Although the data was exaggerated in order to stress the system, the results were very important for further studies that may be conducted. In particular, when using the intact porosity table method, appreciable devaluation in recovery factor (about 12.8% in case 2 and 6.8% in case 1) was obtained due to a substantial decrease in formation permeability caused by rock compaction. When comparing the two way coupling results of case 1 and case 2 with each other, it was noticed that the Kozeny-Carmen and Polynomial Law methods have very similar outcomes in terms of subsidence devaluation percentage, recovery factor percent decrease and pressure at the end of production. On the other hand, we were not able to compare the results obtained using the intact porosity table since the same lab data was used for both reservoir cases even though they are under different conditions, due to lack of data.

Concerning the effect of different techniques on subsidence results, the geomechanical results obtained using the different two way coupling simulations resulted in a devaluation in surface subsidence intensity compared to the one way coupling results. The reason behind this is that the less the production due to decrease in permeability, the more the remaining gas in place and the less the imposed pressure drop, thus the less the reservoir rock displacement.

In conclusion, the one way coupling method is proven to be a very important tool for subsidence calculation since it is a simple, more efficient method in terms of necessary input parameters and computational time ^[15]. On the other hand, two-way coupling could also be an important tool to be used in certain cases and reservoirs, but in our cases the Kozeny-Carmen and polynomial law method showed that even with the two way coupling approach the production data were not severely altered. Contrarily, when using the intact porosity table significant changes in production and pressure results took place. Furthermore, the lab data used as an input for both cases, even though realistic, is not necessarily compatible with the conditions of our reservoir. For this reason, further lab tests on reservoir formations such as loose sand and unconsolidated sandstone should be done. Unfortunately, these test are hard to conduct on such formations since it is hard to extract intact samples from the reservoir without altering its conditions.

References:

- [1] Antonin Settari (1998). A Coupled Reservoir and Geomechanical Simulation System. SPE Journal. Retrieved from www.onepetro.org
- [2] G. Brighenti, P. Macini, E. Mesini (2001). Subsidence Induced by Offshore Gas Production in the Northern Adriatic Sea. Retrieved from www.onepetro.org
- [3] O. Robertson, G. V. Chilingar , L. F. Khilyuk & B. Endres (March 2012) The Environmental Aspects of Oil and Gas Production Subsidence
- [4] A. Settari (2001). Advances in Coupled Geomechanical and Reservoir Modeling With Applications to Reservoir Compaction. SPE Journal. Retrieved from www.onepetro.org
- [5] J.P. Davies (1999). Stress-Dependent Permeability: Characterization and Modeling. SPE Journal. Retrieved from www.onepetro.org
- [6] Andy Merxhani (July 2016). An introduction to linear poroelasticity
- [7] H.Y. Chen, L.W. Teufel, R.L Lee (October 1995) Coupled Fluid Flow and Geomechanics in Reservoir Study –I. Theory and Governing Equations. Retrieved from www.onepetro.org
- [8] Retrieved From www.software.slb.com across
- [9] David Tran (2002). New Iterative Coupling Between a Reservoir Simulator and Geomechanical Module. SPE Journal. Retrieved from www.onepetro.org
- [10] Philip H. Nelson (May-June 1994). Permeability-Porosity Relationships in Sedimentary Rocks. Retrieved from www.onepetro.org
- [11] J.DU, R.C.K. Wong (December 2007). Application of Strain-Induced Permeability Model in a Coupled Geomechanics-Reservoir Simulator Retrieved from www.onepetro.org
- [12] Visage 2015 technical description manuel
- [13] Patrick Baud, Philip Meredith, Edward Townend (May 2012). Permeability evolution during triaxial compaction of an anisotropic porous sandstone. Retrieved from www.onlinelibrary.wiley.com
- [14] Geomechanics in reservoir simulation. Retrieved from www.petrowiki.org
- [15] Grazia Giani, Serena Orsatti, Costanzo Peter, Vera Rocca (may 2018) A Coupled Fluid Flow – Geomechanical Approach for Subsidence Numerical Simulation